AFCRC
TR-56-274

UNIVERSITY OF WISCONSIN
DEPARTMENT OF METEOROLOGY

1956

ENERGY BUDGET STUDIES AT THE EARTHS SURFACE AND DEVELOPMENT OF THE SONIC ANEMOMETER FOR POWER SPECTRUM ANALYSIS

by

V. E. SUOMI

The research reported in this document has been sponsored in part by the Geophysics Research Directorate of the Air Force Cambridge Research Center, Air Research and Development Command, under Contract No. AF 19(122)461

"ENERGY BUDGET STUDIES AT THE EARTH'S SURFACE AND DEVELOPMENT OF THE SONIC ANEMOMETER FOR POWER SPECTRUM ANALYSIS"

by
V. E. Suomi

UNIVERSITY OF WISCONSIN
DEPARTMENT OF METEOROLOGY

Errata

To add on front page ASTIA number: AD 117,197

To add on inside cover the date: April 1957

ABSTRACT:

Page 1, line 9, controvery to controversy

Part I: Heat and Energy Budget of the Lower Atmosphere

Page 31, Line 17, B_o to G_o

Page 32, Line 24, B_o to G_o

Pages 42, 44, 46 and 48, the headings of columns 3, 4, and 6, should read: G_o; Bowen ratio β and A respectively.

Page 50, the headings of columns 3, 4, 5, and 7 should read: G_o; $\beta_{10-33\,cm}$; $\beta_{33-100\,cm}$ and A respectively.

Part II: Power Spectrum of Sonic Anemometer Wind and Sonic Temperature Measurements

Page 5, Line 8, Barrett (1949, to Barrett (1949))

Page 14, $2D_1$; to D_1

AFCRC
TR-56-274

UNIVERSITY OF WISCONSIN
DEPARTMENT OF METEOROLOGY

ENERGY BUDGET STUDIES AT THE EARTHS SURFACE AND DEVELOPMENT OF THE SONIC ANEMOMETER FOR POWER SPECTRUM ANALYSIS

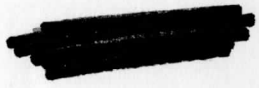

by

V. E. SUOMI

April, 1957

The research reported in this document has been sponsored in part by the Geophysics Research Directorate of the Air Force Cambridge Research Center, Air Research and Development Command, under Contract No. AF 19(122)461

ABSTRACT:

This report summarizes the work done on Air Force Contract AF19(122)-461 which covers studies of the heat and energy budget of the lower atmosphere. The first section covers measurements obtained from a consideration of energy balance at the earth air interface. From measurements of net radiation, heat conduction into the soil and moisture and temperature differences over a small height interval, evaporation and heat added to the air are obtained via the Bowen ratio. The controvery relative to the validity of the Bowen ratio method, since it implies equal eddy transfer coefficients for heat and moisture, is reviewed. Indirect evidence is presented to show provided that the temperature and moisture gradient measurements are made near the surface and provided that the principal sources of heat and moisture are not widely separated compared to the scales of the turbulent motion, the terms of the heat budget which result from application of the Bowen ratio technique are in good agreement with direct measurements of heat added to the atmosphere as determined from bi hourly airplane and radio sonde soundings and are also consistent with the time honored assumption that the eddy fluxes of heat and moisture are constant with height in the surface layer. Evidence is presented to show when sources of heat and moisture are separated on a scale comparable to the turbulent motion, the Bowen

ratio technique is not applicable. It is suggested that the conflicting experimental results, which have appeared in the literature, as to whether or not $K_H = K_V$ may have resulted due to differences in the experimental surfaces in regards to the points on surface uniformity just mentioned. In the discussion of the instrumentation used for the heat budget studies, special emphasis is placed on the requirement that the apparatus used for obtaining hourly moisture and temperature gradients be recorded in a manner that obeys Shannon's sampling law. This can be done by using sensors which have slow speed of response and by sampling at least twice as often as the highest frequency component the sensor will reproduce. Details on the instruments for the measurement of soil heat flow and a net radiation integrating recorder are also given.

The second section describes the theory and constructional details of a sonic anemometer, whose development was completed under the contract. The anemometer measures the space average component of the wind along the axis of the acoustic array. Its output is linear on each side of zero with an error less than 2% when the total wind is less than 50 MPH. The record obtained is a variable area 39 (or 16) mm film similar to a motion picture variable area sound track. A sonic thermometer unit which will obtain a temperature similar

to the virtual temperature is also described. However, due to second order terms, fluctuations of temperature obtained with this instrument are reliable only when the total wind fluctuation is less than 5 m/sec.

Finally methods of power spectrum analysis from the variable area record film are described. The most satisfactory method according to our experience is obtained from an analog computation of the auto correlation function or cross correlation function and a digital evaluation of the Fourier Cosine transform into variance or co-variance spectrum.

In an Appendix, circuit and construction details of the sonic anemometer and thermometer are given.

B PUBLICATIONS:

1. Suomi, V. E. - The Heat Budget over a Cornfield Ph.D. Thesis - University of Chicago - 1953

2. Suomi, Franssila and Islitzer, An Improved Net Radiometer, Jour. of Meteor., Vol. 11, 1954

3. Summary of observation at O'Neill, Nebraska for general observation periods.

4. Summary of observation at O'Neill, Nebraska for standby observation periods.

FOREWORD

This report summarizes the work done on Air Force Contract AF19(122)-461 which covers studies on the heat and energy budget of the lower atmosphere. A considerable fraction of the work is concerned with instrumentation and measuring techniques. Included in this report are those sets of observations and analysis which have not been published elsewhere. Observations such as those obtained during the great Plains Project at O'Neill, Nebraska, not yet published, have not been included since they will be published as part of the O'Neill Project Summary.

It is a pleasure to acknowledge the contributions of all of the personnel participating in the project. While it is impossible to cite individual contributions, the following individuals, who were at the University of Wisconsin part of the time, deserve special mention. Dr. Matti Franssila, Director, Finnish Weather Bureau, Helsinki, Finland; Dr. Eiichi Inoue, Institute of Agricultural Sciences, Tokyo, Japan; Dr. Arnold Glaser, Texas A & M College, Bryan, Texas, and our former students, Mr. Norman Islitzer, Idaho Falls, Idaho; Mr. Jack Schuetz, Illinois State Water Survey, Urbana, Illinois; Mr. Lee Sims, Institute of Atmospheric Physics, Tucson, Arizona, and Mr. William P. Lowry, State Conservation Department, Salem, Oregon. We also wish to credit Mr. Cho-Ching Lee; Mr. Den J. Li and Mr. Gerald Peterson as those who also aided in the labor of the data analysis and Mr. Ernest Romare, Machinist, who constructed some of the apparatus.

HEAT AND ENERGY BUDGET OF THE LOWER ATMOSPHERE

Introduction:

The kinetic energy of the atmosphere is derived from solar energy and is ultimately dissipated via turbulence and viscosity as friction. A major fraction of these energy transformations occurs at the earth's surface with the atmosphere and the surface acting together as the boiler of a heat engine whose working substance is moist air. Research in this field has proceeded along four main directions. (1) Energy budget studies where each term comprising energy balance at the earth's surface is measured independently or as nearly independently as possible, (2) Mass, energy, and momentum transfer studies based on mean vertical profiles of wind, temperature, moisture or other air properties in a manner analogue to, but not identical with molecular transfer of these same properties, (3) Intimate structure studies where fine scale fluctuations of air properties measured with rapid response sensing elements are multiplied by the appropriate component of the instantaneous wind and (4) Studies which include the effects of friction on the equations of motion. The measurements reported on in this report can be classified under item (1) The energy balance of the surface layer and under (3) The structure of the vertical wind.

The energy balance of a volume one face of which is the earth's surface is shown in figure 1.

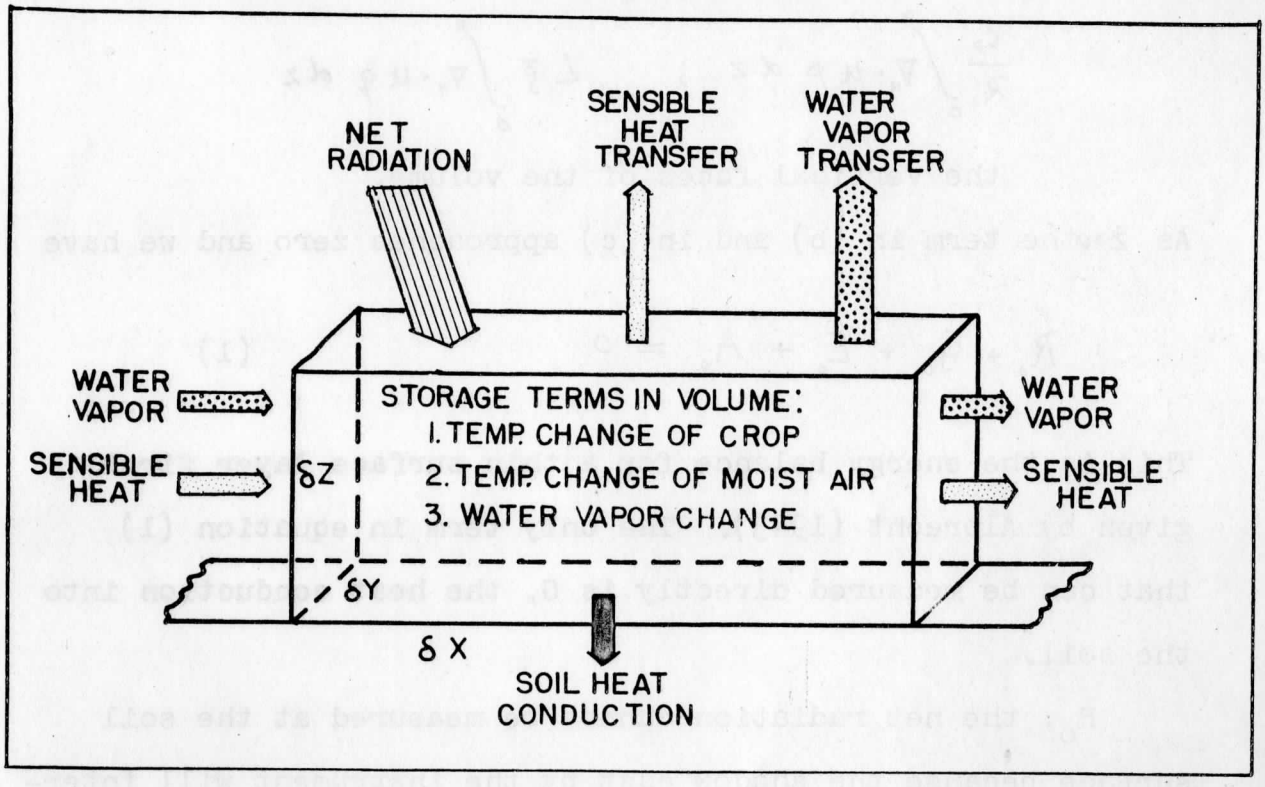

Fig. 1

1. The various terms can be arranged into three groups.

(a) Vertical heat budget terms. There are

$$R_o + G_o + A_o + E_o = 0 \qquad (1)$$

(b) Storage terms. These represent the energy required to change

$$\int_0^z \int_0^t L \bar{\rho} \frac{\partial q}{\partial t} \, dz \, dt \; ; \qquad \int_0^z \int_0^t c_p \bar{\rho} \frac{\partial T}{\partial t} \, dz \, dt$$

the temperature or moisture concentration within the volume.

(c) Divergence terms. These represent heat and moisture flux through

$$\frac{c_p}{R}\int_0^z \nabla_H \cdot u p \, dz \; ; \qquad L\bar{\rho}\int_0^z \nabla_H \cdot u q \, dz$$

the vertical faces of the volume.

As $z \to 0$ the term in (b) and in (c) approaches zero and we have

$$R_o + G_o + E_o + A_o = 0 \qquad (1)$$

This is the energy balance for a thin surface layer first given by Albrecht (1943). The only term in equation (1) that can be measured directly is G, the heat conduction into the soil.

R_o, the net radiation cannot be measured at the soil surface because the shadow cast by the instrument will interfere with the measurement. The radiation instrument used in these experiments was mounted 3 meters above the surface. When there is a strong temperature lapse or a shart inversion near the surface, there will be a divergence of radiation between the surface and the instrument. A radiation chart calculation shows that the divergence is about .5% of the net radiation on a clear day. This same absolute error may be up to 5% of the net radiation measured during a clear night. Except for the small error due to divergence, the net radiation can be measured with very good accuracy. This is indeed fortunate, since it is the largest term of the heat budget.

There is no way to evaluate the terms A_o and E_o directly at the surface. The evaporation term E_o can be evaluated by measuring the mass change due to the water loss in a fixed volume of the soil below the surface. This is not a convenient measurement but it can be done by isolating a volume of the soil so it can be weighed. The heat added to (or subtracted from) the air then remains as a residue from measurements of R_o, G_o and E_o. The data presented for September 2, 3, 4, 5 of 1952 has a complete set of these measurements. A much more convenient, but not as fundamental method of separating A_o and E_o makes use of the Bowen ratio. When K_V is assumed to be equal to K_H the ratio of A to E is proportional to the gradients of temperature and moisture. It is then possible to solve the heat budget ignoring storage and divergence terms from measurements of net radiation, heat conduction into the soil and temperature and vapor pressure gradients.

Pasquill (1949) obtained the heat budget from measurements of R_o, G_o and E_o. He did not, however, measure the net radiation term directly but obtained it from measurements of net shortwave radiation and calculations of long wave balance. From measurements of the temperature and moisture gradient in addition to R_o, G_o and E_o, he obtained the eddy diffusion coefficient by K_V and eddy conduction coefficient K_H essentially as follows:

$$K_H = \frac{R_o + G_o + E_o}{\frac{\partial T}{\partial z}}$$

and

$$K_V = \frac{E_o}{\frac{\partial q}{\partial z}}$$

He found that K_H K_V under unstable conditions contrary to what is assumed for the Bowen ratio. The assumption that K for heat, K_H, equals K for momentum, K_M, has been challenged on theoretical grounds by Ertel (1942) and Priestly and Swinbank (1947). This also implies that K_H does not equal K_V. Swinbank (1955) states that he has proved this inequality experimentally. He used a different technique than that used by Pasquill. He measured the fluctuations of vertical wind, temperature, and vapor pressure. Mean products of the wind and temperature, and wind and vapor pressure yield the heat and moisture transport.

$$A = \bar{\rho}\, c_p\, \overline{w' T'} \qquad (2)$$

$$E = \bar{\rho}\, L\, \overline{w' q'} \qquad (3)$$

Since a mean product can be written in terms of the root mean square values and their correlation coefficient, we can write (2) and (3) as

$$A = \bar{\rho}\, c_p\, \underline{w'}\, \underline{T'}\, r_{wT} \qquad (4)$$

$$E = \bar{\rho}\, L\, \underline{w'}\, \underline{q'}\, r_{wq} \qquad (5)$$

where the bar under the term indicates the RMS value. When $r_{wT} = r_{wq}$ we have the equivalence of $K_H = K_V$. Swinbank found that r_{wT} was positive and systematically greater than r_{wq} during unstable conditions and negative but systematically greater than r_{wq} during stable conditions. In opposition to this view Businger (1954) mentions a discussion by v.d. Held (1947) which contains an argument in favor of $K_H = K_V$. Experimental data obtained by Rider and Robinson (1951) show that $K_H = K_V$. Actually, they compare measurements which when evaluated assume that $K_V = K_M$ as suggested by Pasquill's measurements. They also have evaluated the heat budget via the Bowen ratio method which, of course, assumes $K_H = K_V$. Since the two methods give essentially the same results, they argue that the two coefficients are equal.

Thus, there is considerable difference of opinion on the validity of the assumption that $K_H = K_V$. The data presented in this report in one case contains direct measurements of net radiation R_o, heat conduction into the ground G_o, and evaporation E_o with the sensible heat A_o, being the residue. Evaporation amounts obtained by direct measurement and evaporation obtained by application of the heat budget using the Bowen ratio assumption are in good agreement in most instances. In another set of measurements taken at O'Neill, Nebraska the heat added to the air obtained by measurement of net radiation R_o, heat conducted into the ground

G_o and Bowen ratio separation of the residue into sensible and latent heat can be compared to that obtained from vapor pressure and wind gradients.

The underlying basis for the argument that the coefficient of conductivity K_H should be greater in unstable conditions, equal to in neutral conditions and less than K_V or K_M in stable conditions is that the positive or negative buoyance exhibited by heated or cooled parcels tends to order a selection to otherwise random motion of the air parcels, (Swinbank 1955). Theories have been developed from the assumption that the total turbulent acceleration is equal to a frictionally derived acceleration and a buoyant acceleration. Beginning from this model Lettau (1949), and Businger (1954), have developed theories which explain the curvature of a log z plot of the vertical wind profile as a function of heat flow. The evidence presented is quite convincing that bouyant accelerations do order a selection to otherwise random motions, particularly at some distance from the boundary. This effect shows up as a departure from the log law.

It is easy to visualize how when momemtum, moisture and temperature fluctuations are not highly correlated, the bouyant accelerations could act as a "Maxwell's Demon" to separate the transport of sensible heat from the transport of water vapor or momentum. On the other hand, when the

fluctuations of the air properties are highly correlated initially, the basis of the separation is not as easy to picture. In any case there is considerable experimental data which shows quite clearly that these effects are progressively less important the nearer one gets to the surface. Near the surface the wind profiles show little curvature. Swinbank's measurements show that K_H and K_V are less different at 1.5 meters than they are at 29 meters. Pasquill states that the numerical value of the Richardson's number, the well known parameter that indicates stability, decreases rapidly as the ground is approached. Thus, there is good evidence that as one approaches the surface, the influence of moderate range of stability and hence separation is reduced.

We now suggest a surface model where the warm (or cool) air parcel is the same as the moist air parcel. Consider a typical earth's surface completely covered with succulent green vegetation. Since there is a more or less random orientation of the leaves, there will be small differences in leaf temperature and vapor pressure from leaf to leaf depending on the angle each leaf makes with the sun and mean wind direction. In the case of full sunlight with little or no wind the leaves which are sources of heat due to absorption of solar radiation are also sources of mositure. We can say with confidence that at the leaf surface the fluctuations in temperature will have a high positive correlation with fluctu-

ations in moisture. Conversely in the case of zero net radiation but with ventilation due to wind, each leaf which is a moisture source must be a heat sink due to wet bulb action. This will result in a high negative correlation between moisture and temperature fluctuations. The intermediate case is also possible. Some leaves might be in the shade of another leaf but exposed to the wind and visa versa. Now, if the scale of the wind eddy is large compared to the leaf size, the moisture added to the air parcel from the shaded and unshaded leaves will increase or decrease simultaneously. Some of the heat supplied to the air parcel from the unshaded leaves will be absorbed by the shaded leaves. The presence of closely interspaced heat sinks amongst the heat sources, reduces the amplitude of the temperature fluctuation, but does not destroy the high correlation between moisture and temperature fluctuations. The situation is somewhat analogous to the addition of two alternating currents of opposite phase. The amplitude is decreased but the phase relationship is either maintained or reversed depending on the respective amplitudes, but not shifted to any angle in between.

Now, consider a field covered with a row crop or a series of beds in a more or less checker board fashion. Ordinarily in daytime conditions the evaporation from the bare soil is very much less than transpiration from the plants. The

plant areas can be considered primarily as moisture sources and they can be either heat sources or sinks, depending on the wind velocity. The uncropped areas will be primarily heat sources. Now, if the scale of the wind eddy is of the same order of magnitude or less than the scale of the cropped spaces, significant amounts of heat will be added at different times than when moisture is added. A high correlation between moisture fluctuation and temperature is therefore unlikely. Under these conditions we would expect the equivalent K_H and K_V applied to the area as a whole to be significantly different.

Whether or not this line of reasoning is valid can be tested experimentally. The cospectrum of temperature and moisture variations should show a minimum at the frequency equivalent to the crop pattern scale of the field. Similarly the quadrature spectrum should show a peak at this same frequency. It is proposed to test this assumption in the near future. A high speed infra red absorption hygrometer and a sonic thermometer will be used.

We now describe an indirect test of this model. The constance of the Bowen ratio with height has been used as a test for $K_H = K_V$. The basis for this contention is the assumption that in the surface layer, heat and moisture transport is constant with height. A constant Bowen ratio

with height implies a constant K_H/K_V with height. Figure 2 shows the Bowen ratios measured between 10 cm and 33 cm and between 33 cm and 100 cm above a field of young corn (maize). The plants were 10 cm in height and space 20 cm from each other in rows spread 100 cm apart.

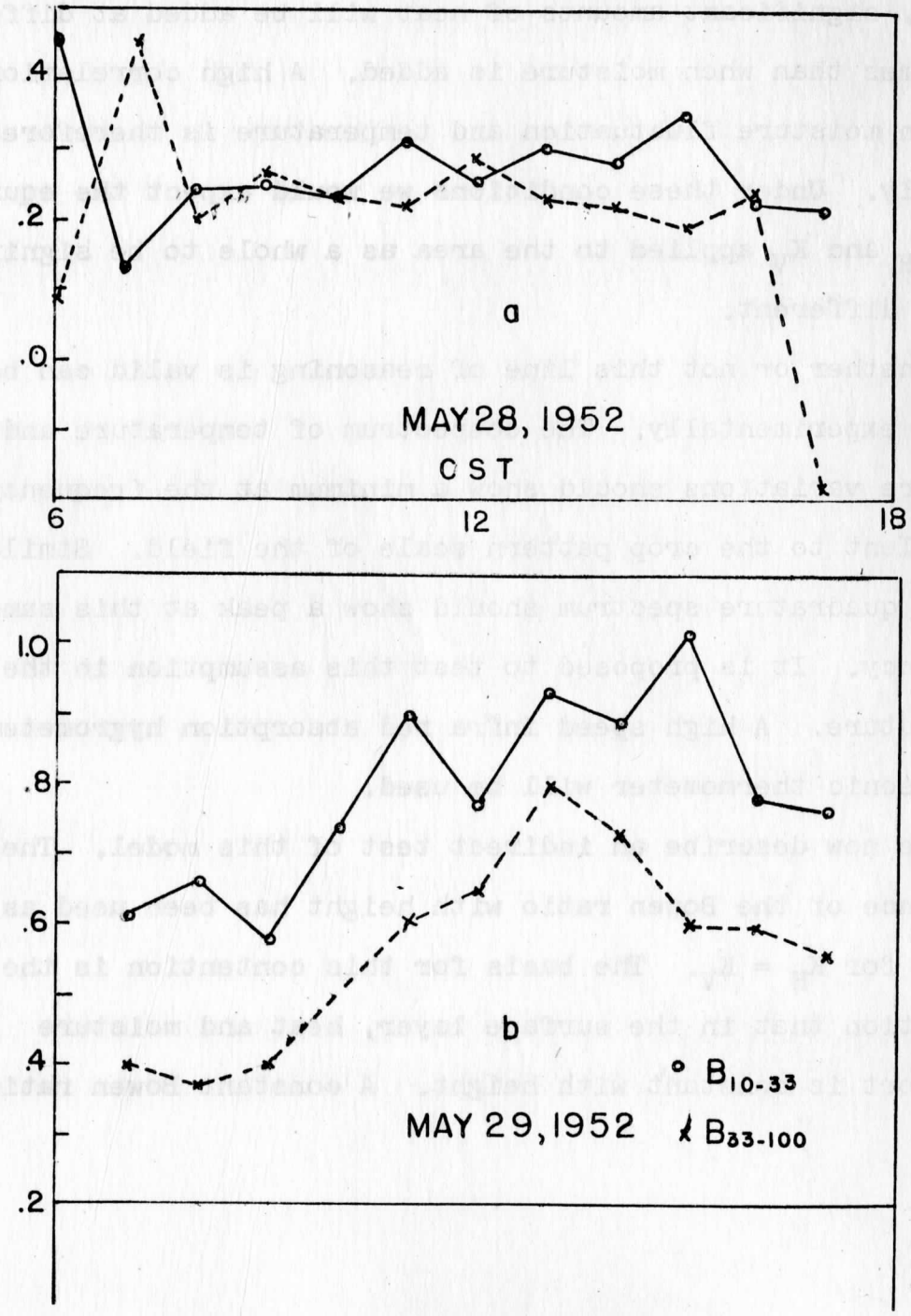

Figure 2

May 28, is a case just after a heavy rain where the soil surface (black peat) was thoroughly wetted. Here, both the soil and the plants are moisture sources. Part (b) of Figure 2 for the next day is the same field after the soil surface had dried out. Here only the plants can be considered a moisture source.

The Bowen ratio is not very reliable near sunrise and sunset since the temperature and moisture gradients from which it is calculated are generally quite small at that time. At other hours the Bowen ratio on the first day with the soil and plants acting as moisture source is fairly constant with height, the departure tending to increase as the day and the drying out of the soil surface progresses. On the next day when the soil surface is primarily a heat source the departure is more striking. The Bowen ratio for the lower level is greater than the Bowen ratio for the upper level. This is entirely consistent with the argument that the departure increases with the elevation as the effects of buoyancy have been shown to increase with distance from the surface. On the other hand when the entire surface is moist K_H/K_V= constant. Here the scale of heat and moisture sources is small compared to the effective eddy size.

One could argue that Pasquill made his measurements near the surface where buoyancy does not have a great effect and still obtained $K_H > K_V$. Pasquill describes the surface

over which he conducted his experiment, "Bare soil was visible over a considerable proportion of the pasture and the patchy grass was mainly 2 cm long with occasional withered tufts up to 5 to 7 cm and showed no appreciable change in length over the whole period of observations." Rider and Robinson describe their surface as " - - - - - - - - or surface of level grass which was kept mown to an average length of 1 to 2 cm,"; and, for Rider's 1954 observations, "A circular area of approximately 250 m diameter was kept mown to a grass length of 2 to 3 cm, ----." It would be presumptious to claim at this stage that the differences in the results of Messrs. Rider and Robinson and of Pasquill are caused mainly by the differences in the surfaces, particularly since the descriptions of each are so brief. We should like, however, to state that in future experiments of this type great care should be given to the selection of a surface. Either a uniform one or a "checker board" one should be chosen so that this aspect of the problem can be considered in more detail.

Swinbank not only describes the surface carefully but includes photos as well. His photos show the grass surface to be rather dry and patchy, at least as far as grass height is concerned. It is not possible to tell from the photos whether or not patches of bare ground existed. Possibly,

part of Swinbank's results which show that near the surface (1.5 and 1.9m) that K_H is greater than K_V may be explained on the basis of the effects of a heterogenous surface. On the other hand, some of it may also be explained in terms of measurement error. The author is very hesitant to criticize the accuracy of Mr. Swinbank's measurements, since he has a very keen appreciation of how difficult this type of measurement is to make and he is particularly hesitant, since he has not himself successfully made measurements of this type to date. Moreover, we are not in disagreement with the general implication of Mr. Swinbank's work, namely, that buoyancy does order a selection on otherwise random motions. We are in disagreement over its magnitude near the surface, particularly its importance over a truly uniform surface.

Table 1 has been extracted from Swinbank's paper for all data at 1.5 or 1.9 meters elevation for which moisture data are also available, that he took since March 3, 1952, when he installed a net radiometer. Data taken before that date have not been included since there is a possibility the net radiation (the largest term in the heat budget) obtained prior to that time may not be as reliable as that taken after. We have changed the volume

TABLE 1

1	2	3	4	5	6	7	8	9	10	11	12
Time	Obs. No.	R	G	L	E	Error	$\frac{\text{Error} \times 100}{R+G}$	r_{wT}	r_{wq}	$r_{wT} - r_{wq}$	$\frac{r_{wT}}{r_{wq}}$
Mar. 3, 1952			mw per cm^2								
14:21	1	46.6	9	19.9	5.8	+ 1.9	31.6	42	24	16	1.75
14:38	3	43.7	8	20.1	3.9	+11.7	32.7	45	18	27	2.5
15:40	5	30.3	3	14.4	3.6	+ 9.3	34.1	47	20	27	2.35
15:57	7	26.9	2	10.9	4.2	+ 9.8	39.3	41	19	22	2.16
17:24	9	4.8	-4	5.4	.69	+ 2.7	337	41	9	32	4.55
17:41		.4	-5	2.8	1.4	+ 1.2	26.1	31	20	11	1.55
18:34		-10.6	-6	- 1.5	- .19	+ 2.9	63.0	-27	-10	17	2.70
18:51	15	-11.3	-6	- 1.4	- .51	+ 3.4	64.1	-33	-23	10	1.43
Mar. 4, 1952											
08:48	47	13.6	3	7	4.3	+ .7	6.6	41	40	1	1.02
Feb. 20, 1953											
07:00	4	- 0.8	-1	0.5	1.03	- .27	150	18	24	6	.75
07:18	5	3.6	0	2.6	4.0	+ 3.0	83	50	42	8	1.19
08:14	8	17.0	4	4.4	4.5	+ 4.1	32	36	31	5	1.16
08:25		20	5	6.8	6.2	+ 2.0	13	53	44	9	1.20
Feb. 23, 1953											
11:40		56	10	14.0	16.0	+16.0	34	47	33	14	1.42
12:01		56	9	16.0	17.5	+14.5	31	46	32	14	1.44
13:00		56	8	8	7.8	+32.2	67	38	22	16	1.72
15:35		33.5	3	8	6.2	+16.3	53	49	26	23	1.88
16:30		20.5	2	6.3	6.9	+ 5.3	29	48	35	13	1.37
18:32		- 7.5	-1	-0.9	+ .76	+ 6.4	98	-40	39	(1)	1.0
20:52		-10	-3	-1.9	+ .52	+ 5.6	80	-37	26	(11)	1.42
21:28		-10.5	-3	-0.9	+ .23	+ 3.67	49	-20	12	(8)	1.66
22:19		-10.5	-3	-1.4	0	+ 6.1	81	-36	1	(35)	
22:42		- 9.9	-4	-0.4	.17	+ 5.67	96%	-19	12	(7)	1.71

indicating mass of moisture loss into equivalent latent heat units to facilitate a heat balance comparison.

The measured values of R_o, G_o, A_o and E_o should add up to zero providing no steady vertical motions exist. Swinbank discusses and estimates the errors which might be present due to any steady vertical motions in the last section of his paper. If the four terms do not add to zero the error which results may be caused by not accounting for any steady vertical motions (which last the 5 minutes observation time) or from deficiencies in the measurement technique itself. Measurement of R_o and G_o should be fairly reliable (easily better than 10%). A_o and E_o can be expressed as the fraction of $R_o + G_o$. If no errors are present this ratio should be unity i.e.

$$\frac{R_o + G_o}{A_o + E_o} = -1$$

it can also be expressed as the percentage error

$$\frac{R_o + G_o + A_o + E_o}{R_o + G_o} \times 100 = \% \text{ error}$$

Column 8 of Table 1 shows this error.

Swinbank uses $r_{wT} - r_{wq}$ as an indicator of the failure of $K_H = K_V$, i.e. if

$$r_{wT} - r_{wq} > 0 \qquad K_H > K_V$$

Figure 3(a) is a plot of the percentage error mentioned earlier, against $r_{wT} - r_{wq}$. Taking all the data of Table 1 into account there is only a slight indication that the magnitude of the difference $r_{wT} - r_{wq}$ is related to the magnitude of the error. On the other hand, if we select all the daytime cases where the radiation and all the other terms of the heat budget are large and presumably easier to measure, these data should be the most reliable of the group. Figure 3(b) is a plot of these selected values (all values where R_o is greater than 10 mw/cm^2/sec). Now a relation between $r_{wT} - r_{wq}$ and the size of the error is much more evident. It appears, therefore, that a significant portion of the data which has been used to show that $K_H > K_V$ near the earth's surface has an error which is proportional to the degree of inequality.

Part of the error could be due to the steady vertical motion term. All of the errors in Table 1 are on the short side, that is Swinbank's eddy motion transfer never is as great as the residue from $R_o + G$. One would think that some steady (5 minute duration) motion would be positive and some negative, thus causing the error to have both signs.

Measurements of the type accomplished by Swinbank are very difficult to make. He has shown that as one

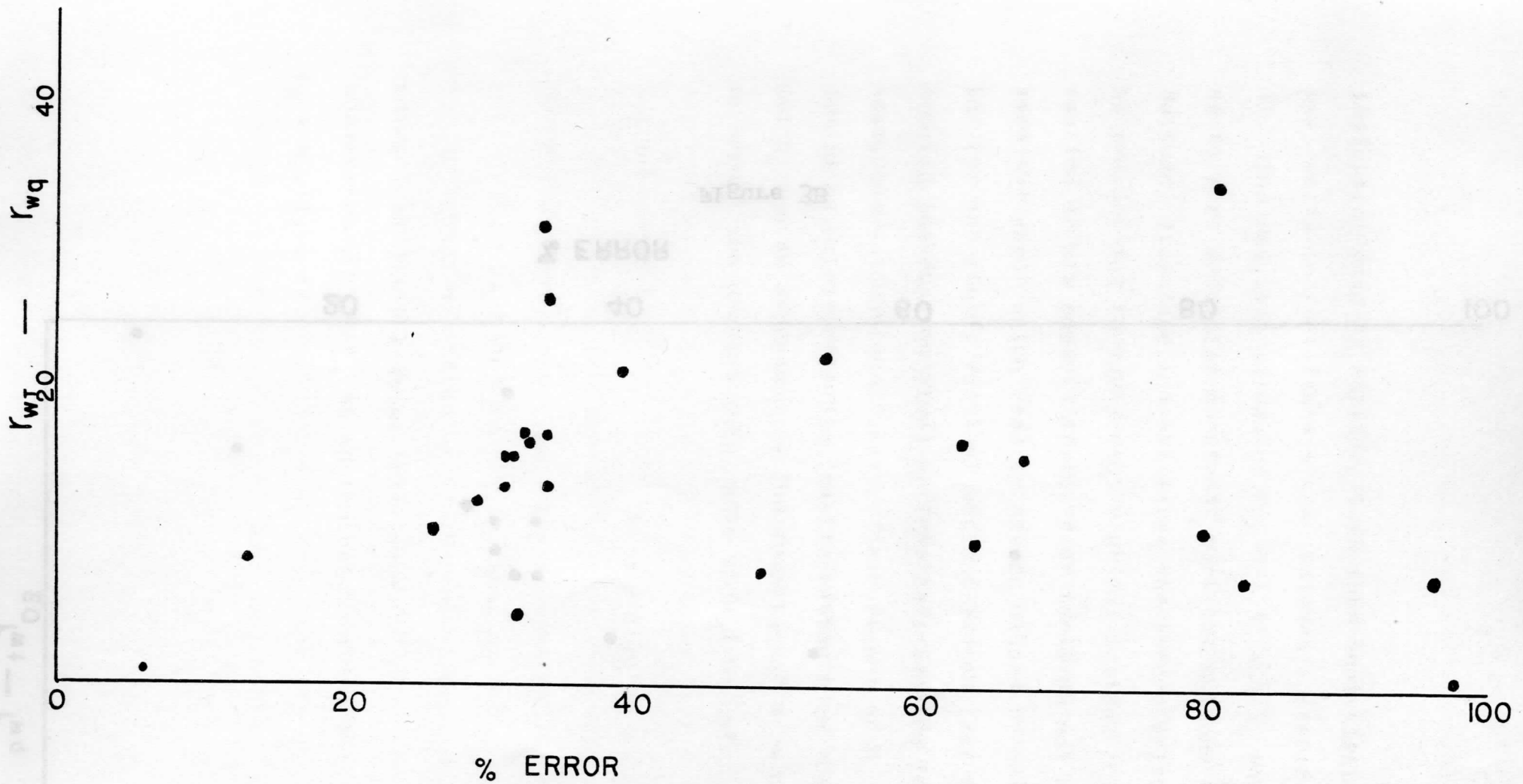

Figure 3A

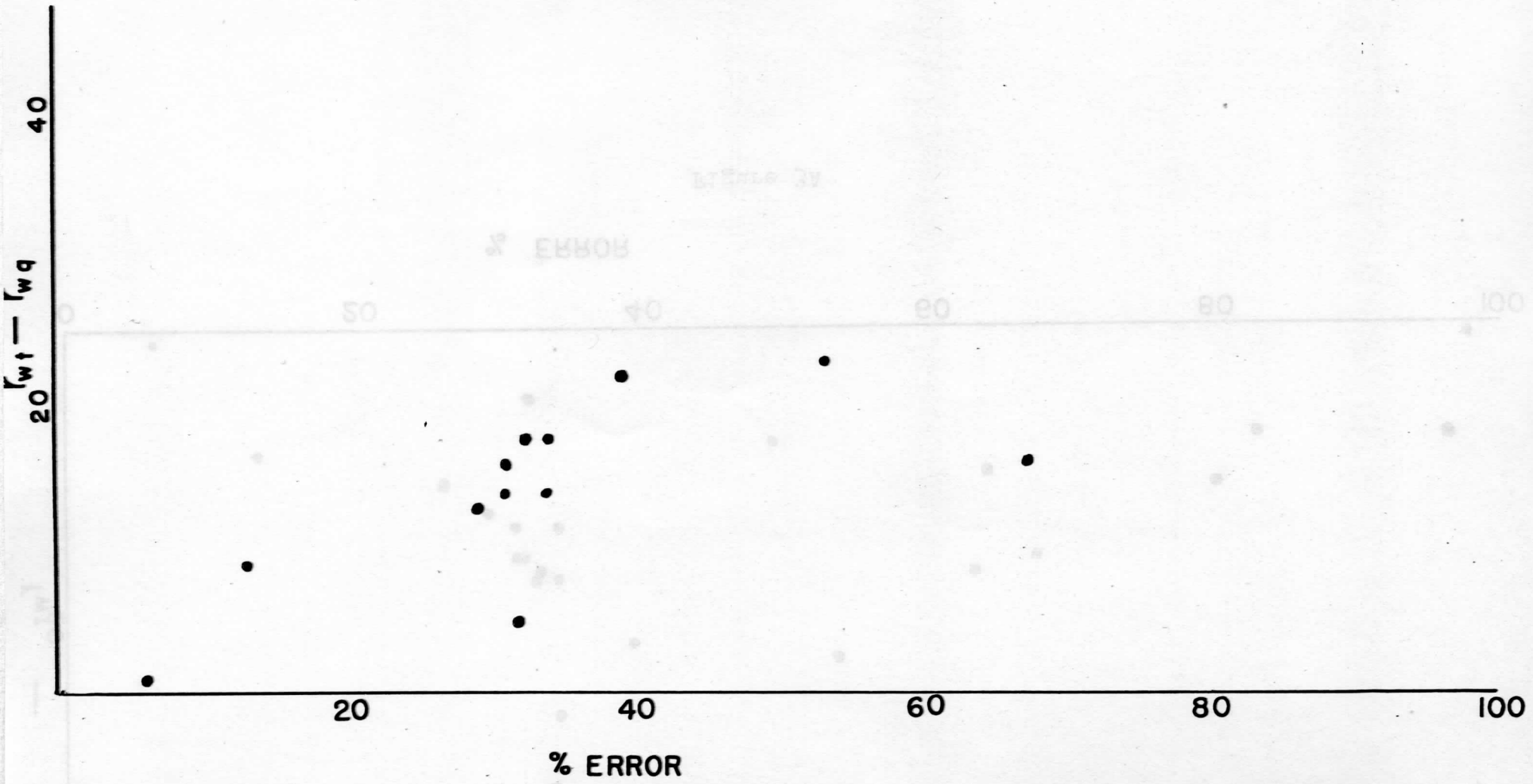

Figure 3B

approaches the surface the effect of buoyancy tends to be reduced. He has also shown that the length of the observation period required for an adequate sample is considerably less than that required at higher elevation. It would appear that in the interest of securing accurate results, measurements should be made as near the surface as possible. Yet, near the surface the frequencies of temperature and wind fluctuation are higher than at upper levels, thus raising the requirement for high fidelity at high frequency in the measuring apparatus. The two effects are antagonistic.

Divergence effects:

If one investigates the spectrum of eddy motions there is ample evidence to show that the scale of turbulent motion covers a vast range from millimeters to kilometers. Expressed as frequency, the fluctuations can vary from many cycles per second to only a few per hour or perhaps even a few per day. These slow, large eddies effect one of the fundamental assumptions in all of the theories that explain turbulent transfer of air properties, namely, the requirement that no mean vertical mass transfer exists, that is

$$\overline{\rho w} = 0$$

This assumption is valid at the earth's surface. It is also met if the horizontal surface is a pressure surface provided the system under investigation has material vertical walls, a situation not true in the open atmosphere.

The assumption is not met if the surface is not flat or does not have uniform thermal properties on a scale comparable with the largest eddies. In fact, we might go as far as to say that the departures of the actual experimental surface from a mathematically uniform surface, may be the cause of the larger eddies. In this regard, the O'Neill, Nebraska site was ideal in that not only was the surface quite flat, but it also had a very uniform surface cover, soil thermal properties and albedo on a very large scale. On the other hand, the University of Wisconsin Marsh Farm site used in the 1952 experiments, while exceptionally flat and uniform for a 80-100 acre site, (even the plants were remarkably uniform) was different from the surrounding area. The water table was only 18-20" below the surface of the field, so that the plant always had an ample moisture supply. The heavy evaporation would tend to make the field cooler than the surrounding area. Thus, it is entirely possible that a sea breeze type circulation was super-imposed on the mean flow.

September 3, 4, and 5, were three clear days in sequence with almost identical amounts of net radiation. The evaporation obtained from heat budget calculations for September 3, and 4, were almost identical yet the measured evaporation obtained from the lysimeter showed a 30% increase on September 4, over that measured for September 3. September 4, was a hot windy day with considerable warm air advection.

The reader will recall that the temperature and vapor pressure gradients were measured about one meter above the corn whose average height was about three meters. Evidently, in this case the divergence terms shown in Figure 1 could be an important additional heat source.

Richardson's number for the midday hours on September 4, is significantly less than for the same hours on September 3, indicating a greater bouyant instability on September 3. One is tempted to conclude that the underestimation of evaporation on September 4, arises from the fact that sensible heat was over estimated because the ratio $\frac{K_H}{K_V}$ was really less on September 4, than on September 3, rather than equal as assumed in the calculations of the heat budget. We find that on September 5, the Richardson's number for 11-12 o'clock observations indicates even less convective instability yet the agreement between

lysimeter measured evaporation and heat budget calculated evaporation is again as good as on September 3, two days earlier. In Figure 13 a chart showing the hourly changes in mean soil temperature, we see that at 001^h on September 4, the soil was the coldest of the three days shown, yet at 2400^h of the same day it was the warmest. Clearly on the day with the greatest soil heating, the greatest measured evaporation, and the maximum change in air temperature, more energy than available from net radiation is required to balance the budget.*

Thus it appears that the problem of whether or not $K_H = K_V$ is still not settled. The precision of measurement required has not yet been reached in those measurement techniques making use of energy balance, nor those using instantaneous values of W, T, and Q. Perhaps the concern over K_H and K_V is from applied micrometeorology standpoint, like kicking a dead horse. A large error in $\frac{K_H}{K_M}$ does not give rise to as large an error in evaporation since in the calculation E is proportional to the quantity $(1 + \frac{K_H}{K_V})$. Horizontal divergence is likely to give much larger errors.

*In another experiment (to be reported on in detail elsewhere) conducted at Hancock, Wisconsin, in 1955, over irrigated alfalfa but where gradients were measured only 10 cm from the crop surface, no divergence effect was obtained. Moreover, the ratio $\frac{E(\text{heat budget})}{E(\text{lysimeter})}$ remains essentially constant over a wide range of Richardson's numbers including both positive and negative Bowen ratios.

The Heat Budget Experiments:

Heat budget measurements were obtained at two different sites: The University of Wisconsin Marsh farm during the summer of 1952 and the O'Neill, Nebbraska site during the summer of 1953. The heat budget measurements were complete during the 1952 experiments in that independent measurements of moisture loss via an evaporimeter were available. On the other hand much more data from other participants is available, from the Nebraska experiments. Unhappily, no direct moisture measurements were possible during this experiment. What follows now is a detailed description of the instrumentation used for the 1952 measurements. The 1953 measurements at O'Neill were for the most part similar to those taken in 1952 except for some improvements in sampling frequency. Details concerning the methods of measurements, accuracy, etc., will be dealt with quite thoroughly in the forthcoming publication from GRD, summarizing the results of the experiment. Figure 4 shows shematic layout of the instruments used in the 1952 series.

(1) Site. The measurements were taken on the University of Wisconsin Marsh Farm. This 120 acre field is exceptionally level, having height variations of only 15 to 30 cm over most of its area. A particular feature of this location

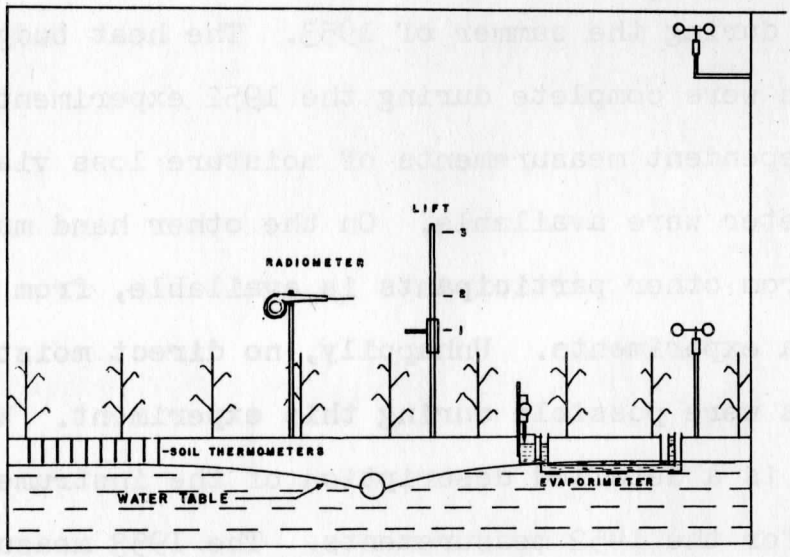
LIFT
3
2
1
RADIOMETER
SOIL THERMOMETERS
WATER TABLE
EVAPORIMETER

Figure 4

is its uniform soil characteristics both with respect to composition and moisture content. The water table is held at a constant level 40 to 30 cm over most of its area. The peat soil provides an ample supply of moisture from below through capillary action, Lokken (1950). Obstructions to wind were one mile to the southwest, three-fourths mile to the south, one-half mile to the west and northwest, one-fourth mile north, and 1,000 feet to the east.

(2) Net Radiation, $R_{(z)}$ The net shortwave and longwave radiation was measured with a net radiation instrument, mounted horizontally at the same height as the Assman psychrometer mast. A complete description of the instrument, method of zero set, calibration method, and accuracy has been given in a paper by Suomi, Fransilla and Islitzer (1953).

(3) Soil Storage, B_o --- The flow of heat into or out of the earth's surface is given by the product of the thermal conductivity and the temperature gradient in the soil boundary soil layers. This simple relationship is not usable because the thermal conductivity of the soil is not a constant. It depends on the soil composition, compaction, and moisture content. This is not the only difficulty. One is forced to obtain the temperature of a two-dimensional surface with

a three dimensional thermometer. Martinelli, et al. (1949) and Deacon (1949) have described heat meters based on this conduction relationship where the temperature gradient existing across a thin sheet of bakelite or glass of constant conduction characteristics is measured with alternate junctions of a thin thermopile. A number of heat conduction plates following the construction described by Deacon were made and embedded at various depths and locations in the soil. Results, however, were not satisfactory. When the plates were mounted near the soil surface as was necessary to account for most of the soil heat flow, they interfered with flow of moisture through the surface and, therefore, with the heat capacity, conductivity, and equilibrium temperature of the soil. On the other hand, if they were set deep enough not to affect the moisture flow, most of the heat transfer occurred above them, thus making it necessary to do calorimetry for that soil layer. Vehrencamp (1953) has used the heat meter method to measure the heat budget of a dry lake bed. Here evaporation and soil moisture changes were negligible. He mounted his last meters only 2 mm below the smooth surface and used a soil and water paste to cement them in position.

The calorimetric method of obtaining B_o requires a measurement of the soil temperature profile and the soil

heat capacity. The heat conduction through the surface can then be obtained from the expression:

$$G_o = \sum_{o}^{z} \rho_s c_s \Delta T \Delta z \qquad (6)$$

where c_s is the specific heat per unit mass and ρ_s is the soil density. Δ T is the temperature change of each layer for the period in question. Eight thermocouples at various depths were set out for a main support similar to the arms of a series of stacked letter E's so as not to disturb the structure of the soil. The soil conduction terms for May 28 - 29 and June 26 - 27 were obtained with this apparatus. It was found necessary to adjust the specific heat of the soil from .74 to .80 to keep from getting inconsistent results in the remainder of the heat budget. Apparently hand cultivation in the immediate vicinity of the temperature probe did not quite duplicate what was done by the farm machinery elsewhere.

Referring to equation (6) one sees that there is not much point in getting a profile of the temperature without at the same time having a profile of the soil heat capacity. It is difficult to sample thin layers of soil so the mean heat capacity for 0 to 7 cm, 7 to 20 cm, and 20 to 30 cm layers were taken. The heat capacity per unit volume for each sample was obtained with an electric calorimeter.

Since the final use of the soil temperature profile is to obtain the average temperature change for the entire layer, it is much simpler to do the actual averaging with a long resistance thermometer element. Better sampling was also obtained by using ten nickel resistance thermometers 30 cm long connected in series with appropriate compensation leads. These elements were set across ten rows, each element representing a different part of the row. The temperature change was obtained from resistance changes which was measured on a Wheatstone bridge. This method of obtaining B_o was the best of three methods tried. Moreover, the equipment was easy to build, calibrate and use. The advantage gained in having a better statistical sample outweighs the error introduced by using the product of the mean temperature and mean soil heat capacity instead of the mean of their product.

After a series of tests in which all three methods of measuring the soil heat conduction term were compared, the soil temperature profile and heat meter methods were abandoned. The data for August 27 - 28 and September 2 - 5 were obtained with the ten resistance thermometers. Hourly measurements of heat capacity were also taken. This method gave an error of 5% of the soil conduction term, thus only 1 to 2% of the total.

Temperature and Moisture Gradient:

Ordinarily, temperature and vapor pressure profiles near the earth's surface are obtained by measuring the difference in temperature of thermocouples set into two or more psychrometers. The use of instruments of similar construction and exposure, together with the difference measurement, tends to eliminate most of the errors in absolute magnitude. However, Pasquill (1949) states that, in spite of care in construction and exposure, enough errors remain to warrant frequent zero checks. Presumably these residual errors are due to differences in wet bulb feeding, imperfect wet bulb performance, dirt accumulation, and spurious thermal e.m.f.'s.

The temperature and vapor pressure gradients for this experiment were obtained with a single psychrometer similar to the one described by Pasquill (1949) mounted on an automatic electric lift. The psychrometer's position was changed from 10 cm to 33 cm to 100 cm, back to 10 cm, and so on every 80 seconds. The 80-second interval gave 14 observations per hour of dry bulb temperature and wet bulb depression for each height. The remaining 60 seconds of the sequencing interval were used to record zero's and the other parameters. It was found helpful to include a reference mark to indicate when the lift was at the bottom position.

With this scheme each measurement had the same wet and dry bulbs, same thermojunctions, same soldered connections, same wires, same relay contacts, same potentiometer recorder, same pen, same chart, same zero check, and approached the reading from the same direction, thus giving the same dead zone error. While this last statement seems to be overemphasizing details, every one of these points could be a source of systematic error which would cause concern when dealing with small gradients.

In addition to the precautions mentioned above, the thermal mass of the dry bulb was adjusted until it had the same time constant as the wet bulb. Spilhaus (1936) has shown that unequal time constants will introduce an error during unsteady conditions.

Apart from the strictly instrumental sources of error, there remains the effect of the fluctuations of temperature and vapor pressure on the accuracy of the hourly means. The large thermal mass of the psychrometer bulbs removed fluctuations whose periods were shorter than ten seconds. However, large fluctuations of a much longer period remained. Shannon (1949) in his development of communication theory, has shown that in order to reproduce completely a signal whose highest frequency has a period τ, it is necessary to take samples at twice the highest frequency or every $\tau/2$ seconds. This requirement was certainly not met in our equipment, nor can it ever be as long

as measurements are made in three places with the same instrument. In order to gather more samples, the time constant must be shortened to allow more rapid adjustment to the new environment. This in turn would increase the band width and would raise the highest frequency of the signal. The two properties are antagonistic. Of course, one can sample rapidly first and integrate later, but the two cannot be combined in one instrument.*

An error analysis of $\Delta T/\Delta z$ and $\Delta e/\Delta z$ for eight hours of data for May 28, 1952 under unstable conditions and four hours of data under stable conditions were carried out by Mr. Norman Islitzer and Mr. Chi-Ling Lee. If the observations at each level are considered independent of each other, the standard error of the mean is about 15 to 20% of the gradient being measured. This represents the maximum error. If the fluctuations at the two levels are related, the error is much less. When the correlation coefficient between psychrometer readings at one level and another equivalent psychrometer of identical characteristics at another level is .9, the standard error of the mean is only 4 to 6% of the gradient being measured. This represents the lower limit of the error. If the correlation is .8, the standard error of the mean is 8 to 10%. It was not possible to establish the correlation coefficient between $T_{10'}$ and $T_{33'}$ and T_{100}

*In the O'Neill experiment this difficulty was eliminated by using two psychrometers mounted on a double lift.

because of having only a single psychrometer. Data presented by Geiger (1950), Gerhardt and Gordon (1948), and Rider and Robinson (1951), indicate that r = .8 is a reasonable value.

Evaporimeter:

The evaporimeter was used to obtain direct measurements of the latent heat flux. It consisted of a tank 20" deep and 60" in diameter, floating in another tank 66" in diameter. The inner tank was filled with earth which held full sized corn plants arranged in rows to simulate the surrounding area. These plants were transplanted about three weeks before the measurements were taken. Whole blocks of earth were moved to prevent disturbing the root system. Rain which packed the earth occurred several times in the three week interval. There was no wilting or other apparent damage to the plants. On the whole the evaporimeter was an excellent sample of the surroundings. It was not possible to distinguish it from the surroundings when viewed from above on a 100-foot tower 100 feet away.

The surface of the water in the "moat" was covered with oil to prevent water loss from evaporation. A Hooke gauge and stilling well enabled the change in mass to be measured from the use of Archimedes' principle. Changes in

the water level could be read to .001 ft. (.3mm) and were estimated to .0001 ft. (.03mm). The resolution of the evaporimeter was not good enough to obtain hourly values of evaporation. However, since the water loss was cummulative, the percentage error was less than 10% for the periods of several hours.

The accuracy of the direct evaporation measurement was not limited by the accuracy of the water level measurement but by the area the evaporimeter was set to represent. This area was <u>not</u> the surface area of the inner tank. Instead, the area was chosen to equal that represented by an equivalent length of plant row held by the evaporimeter.

The data for the 1952 heat budget series is tabulated in tables 2 - 5. The headings of the columns are self explanatory. Another summary of the data is shown in figures 5 to 13. Note that negative values of G_o, A_o and E_o have been plotted in order to save space. The values of energy tabulated for net radiation exchange and soil storage in the tables and diagrams that follow can be considered quite reliable. This is especially true of the August and September data where a superior model of the net radiation instrument was used. These data have been corrected for a small error due to variability of the absorption coefficient with wave length. The soil term

for these data was also under finer control because of the method of sampling and the frequent heat capacity determination. The least precise part of the measurements was the determination of the gradients of temperature and vapor pressure especially at night when they were small.

Measurements in every case were made at two heights in order to test whether or not the Bowen Ratios were constant with height. During the May observations the plants were 8 - 11 cm high, spaced 20 cm apart, in north south rows, 1 meter apart. On July 19, the plants were 30 cm high.

By late August the corn was full grown, and a new lift and psychrometer with stops at 237 cm, 342 cm, and 484 cm, above the soil was necessary to get the measurements above the corn crop. At this time very little sunlight reached the soil (except for 20 minutes during local noon) so that a rough but uniform surface was present. The lowest psychrometer level 237 cm above the soil, was about the same height as the corn tassels and was effected by the presence of nearby plants. In some cases the lower gradient actually reversed sign. Apparently, it is necessary to take both space and time means when working near an inhomogeneous surface. At night i.e., during the time

that the net radiation was negative, the lowest gradient measured at 237 to 342 cm was used for the Bowen Ratio, since the uppermost one was generally very small. During the day the gradient measured from 342 to 484 cm was used. This change is indicated in the table by the horizontal bar.

TABLE II

HEAT BUDGET OVER UNIVERSITY OF WISCONSIN
MARSH FARM CORNFIELD

Time	T_o	B_o		E	L	T_o°C.	T°C.
Sept. 2							
1000-1105	405	38	.78	206	161	16.4	14.3
1105-1200	334	26	.45	212	96	16.8	14.2
1200-1300	340	- 4	.68	205	139	16.8	14.6
1300-1400	203	-14	.53	142	75	16.6	14.6
1400-1500	205	-20	.64	137	88	16.2	14.2
1500-1600	144	-26	.65	103	67	16.0	13.7
1600-1700	112	-38	.16	129	21	15.8	13.0
Sept. 3							
0200-0300	-64	-26	1.04	-18	-20	14.1	11.9
0300-0400	-80	-26	.52	-35	-19	14.7	12.0
0400-0500	-91	-32	.77	-33	-26	14.7	12.0
0500-0600	-110	-40	.51	-46	-24	14.6	12.6
0600-0700	60	-20	.28	62	18	14.9	13.5
0700-0800	263	14	.74	143	106	15.5	14.3
0800-0900	452	44	.61	252	256	15.9	14.5
0900-1000	610	80	.99	266	264	16.0	14.8
1000-1100	695	106	.81	324	265	16.7	14.4
1100-1200	721	148	.53	374	199	19.8	15.6
1200-1300	684	94	.76	334	256	20.6	16.9
1300-1400	598	30	.69	336	232	19.0	17.6
1400-1500	462	6	1.05	222	234	20.4	18.0
1500-1600	287	-20	.57	191	116	18.9	18.5
1600-1700	102	-32	.57	85	59	17.4	18.5
1700-1800	- 54	-48	.8	4	-10	16.2	17.7
1800-1900	-121	-72	2.6	-13	-36	15.1	13.6
1900-2000	-107	-110	1.9	1	2	14.4	12.5
2000-2100	-106	- 72	2.2	-10	-24	14.1	12.7
2100-2200	-106	- 48	2.8	-15	-43	14.3	12.9
2200-2300	-100	- 40	1.8	-21	-39	14.3	12.6
2300-2400	-104	- 38	1.5	-26	-40	14.3	12.4

TABLE II ----Continued

mb	T C.	mb	u M/sec.	u M/sec.	$\frac{u_{30M.}}{u_{1\ M.}}$	dd	Cloud	
10.5	-0.28	-0.23	3.05	6.02	1.97	NW	8	Sc
10.6	-0.31	-0.44	2.77	5.25	1.90	NW	9	Sc
10.6	-0.20	-0.19	3.02	6.00	1.99	WNW	9	Sc
10.7	-0.10	-0.12	2.78	5.63	2.02	WNW	10	Sc
10.5	-0.12	-0.12	3.22	6.69	2.07	WNW	10	Sc
10.5	-0.06	-0.06	3.25	6.50	2.01	WNW	10	Sc
10.7	-0.01	-0.04	3.07	6.08	1.98	WNW	10	Sc
11.6	.13	.08	1.73	3.32	2.26	NW	9	Sc
12.1	.30	.37	1.37	3.02	2.64	NW	9	Sc
12.6	.41	.34	1.46	4.15	2.85	NW	3	Sc
13.3	.22	.28	1.18	3.32	2.82	NW	1	Ci
13.8	.13	.30	1.36	3.20	2.34	NW	1	Cu
13.7	-.15	-.13	1.65	3.55	2.16	NW	1	Cu
12.8	-.17	-.18	1.62	3.25	2.01	NW	0	--
11.2	-.37	-.24	1.83	3.83	1.82	NW	0	--
9.8	-.57	-.45	1.52	2.81	1.84	NW	0	--
9.9	-.29	-.35	1.55	3.04	1.95	NW	0	--
10.1	-.40	-.34	2.04	4.18	2.05	NW	0	--
10.4	-.40	-.37	1.29	2.87	2.24	NW	0	--
10.5	-.33	-.20	1.71	2.78	1.62	NW	0	--
10.9	-.32	-.36	1.16	2.53	2.20	NW	0	--
11.0	-.08	-.09	1.48	2.71	1,80	NW	0	--
11.5	.05	.04	----	2.10	----	W	0	--
13.1	.73	.18	----	1.54	----	W	0	--
12.4	1.83	.62	----	1.44	----	W	0	--
12.0	1.68	.50	----	2.09	----	W	0	--
11.9	.78	.18	----	2.85	----	W	0	--
11.5	.57	.20	.85	3.75	----	W	3	Ci
11.4	.57	.24	.81	3.22	----	SW	3	Ci

TABLE II ----Continued

Time	E_o	B_o		E	L	T_o°C.	T°C.
Sept. 4							
2400-0100	-104	-36	2.5	-21	-47	14.2	12.2
0100-0200	-104	-30	1.8	-23	-41	14.2	12.3
0200-0300	-102	-30	1.5	-29	-43	14.2	12.2
0300-0400	-100	-32	1.3	-29	-38	14.2	12.0
0400-0500	-102	-41	1.6	-23	-38	14.2	11.8
0500-0600	- 95	-32	1.4	-26	-37	14.1	12.4
0600-0700	36	16	.56	13	7	14.2	13.8
0700-0800	254	44	.27	165	45	15.0	16.0
0800-0900	443	80	.70	218	152	15.8	17.1
0900-1000	578	118	.61	286	174	16.1	18.5
1000-1100	666	142	.54	340	184	16.7	19.6
1100-1200	709	140	1.23	255	314	20.4	20.5
1200-1300	691	74	.63	379	238	22.1	21.5
1300-1400	596	40	.49	373	183	19.8	22.2
1400-1500	456	14	.75	252	190	21.4	22.8
1500-1600	289	- 4	.27	230	63	19.9	23.0
1600-1700	110	-24	.04	12	112	17.9	22.7
1700-1800	-60	-41	-1.86	21	-39	16.8	21.5
1800-1900	-120	-46	7.27	- 9	-65	15.8	18.9
1900-2000	-116	-40	5.3	-12	-64	15.3	17.2
2000-2100	-119	-38	2.1	-26	-55	15.3	17.2
2100-2200	-118	-32	0.0	----	-----	-----	17.2
2200-2300	-121	-30	3.7	-18	-72	----	15.9
2300-2400	-119	-28	1.2	-40	-51	----	15.8
Sept. 5							
2400-0100	-116	-44	1.55	-28	-34	----	15.7
0100-0200	-118	-30	1.28	-38	-50	----	15.9
0200-0300	-115	-34	1.05	-39	-42	----	15.2
0300-0400	-107	-40	.91	-35	-32	----	14.5
0400-0500	-105	-32	.71	-42	-31	----	14.4
0500-0600	- 75	-12	.95	-33	-30	----	13.8
0600-0700	83	-20	.93	33	30	----	15.5
0700-0800	281	40	.16	204	37	----	17.3
0800-0900	470	50	.26	334	86	----	19.6
0900-1000	609	76	.71	312	219	----	21.9
1000-1100	687	116	.33	428	143	----	23.4
1100-1200	717	130	.27	463	124	----	24.7

TABLE II ----Continued

mb	T°C.	mb	u M/sec.	u M/sec.	$\frac{u_{30M.}}{u_{1 M.}}$	dd	Cloud	
11.2	.58	.15	.87	3.45	3.94	SW	1	Ci
11.1	.60	.22	.73	3.12	4.22	SW	1	Ci
11.1	.52	.22	.74	3.21	4.35	SW	0	—
11.1	.65	.32	.65	3.10	4.75	SW	1	Ac
11.2	.54	.21	.59	2.97	5.00	SW	0	—
11.6	.39	.17	.86	3.16	3.65	SW	0	—
12.3	.05	-.07	.99	2.76	2.79	SW	0	—
13.0	-.03	-.07	.93	2.55	2.73	SW	0	—
12.8	-.24	-.22	1.63	3.86	2.38	SW	0	—
13.1	-.20	-.21	1.81	3.26	1.81	SW	0	—
13.4	-.31	-.37	2.35	3.90	1.66	SSW	0	—
13.4	-.19	-.10	2.50	4.06	1.62	SSW	0	—
14.1	-.39	-.40	1.92	3.28	1.71	SW	0	—
12.6	-.20	-.26	2.45	3.78	1.72	SW	0	—
12.7	-.13	-.11	2.28	3.81	1.68	SW	0	—
12.8	-.11	-.26	2.14	3.61	1.69	S	0	—
13.3	-.01	-.17	----	----	1.81	S	0	—
14.4	.26	-.05	----	----	2.70	S	0	—
14.4	.80	.07	.76	3.86	5.03	S	0	—
14.2	.91	.11	.71	2.60	3.57	S	0	—
13.8	.05	.12	2.10	4.04	1.92	S	0	—
13.4	.32	.26	2.2	4.06	1.84	S	0	—
13.1	.29	.05	1.73	3.47	2.00	S	0	—
13.0	.38	.21	1.86	3.62	1.94	S	0	—
12.7	.12	.05	2.05	3.82	1.84	S	0	—
12.6	.34	.17	----	----	----	S	0	—
12.8	.36	.22	2.19	3.95	1.80	S	0	—
12.5	.44	.31	1.28	3.08	2.40	S	0	—
12.4	.39	.34	1.60	3.32	2.07	S	0	—
12.4	.47	.32	1.32	2.86	2.17	S	0	—
12.5	.48	.33	2.37	3.92	1.66	S	0	—
12.9	-.02	-.08	2.91	4.80	1.65	S	0	—
14.0	-.04	-.10	----	----	----	S	0	—
15.0	-.11	-.10	3.30	5.08	1.54	S	0	—
16.3	-.13	-.25	3.58	5.65	1.58	S	0	—
17.0	-.17	-.41	3.64	6.05	1.67	SW	0	—

TABLE III

HEAT BUDGET OVER UNIVERSITY OF WISCONSIN
MARSH FARM CORNFIELD

Time	R_o	B_o		E	L	T_o°C.	T°C.
August 27							
1500-1600	431	-17	-0.05	472	-24	29.8	29.2
1600-1700	214	-19	-0.08	248	- 8	28.6	28.6
1700-1800	30	-36	-0.23	88	-22	26.9	27.3
1800-1900	-63	-71	-0.39	13	- 5	25.9	25.4
1900-2000	-73	-48	-1.10	-12	-13	25.0	24.1
2000-2100	-67	-48	-5.60	4	-23	24.5	23.3
2100-2200	-65	-48	-1.93	18	-35	24.2	22.5
2200-2300	-68	-36	-----	---	---	23.9	21.5
2300-2400	-74	-31	-----	---	---	23.8	22.3
August 28							
2400-0100	-74	-33	----	---	---	23.7	22.1
0100-0200	-40	-28	----	---	---	23.6	----
0200-0300	-47	-28	----	---	---	23.6	20.2
0300-0400	-33	-42	----	---	---	23.3	20.2
0400-0500	-38	-42	----	---	---	23.3	20.8
0500-0600	-48	-28	----	---	---	23.3	20.0
0600-0700	54	42	-0.64	35	-23	23.1	21.1
0700-0800	154	50	0.11	94	10	23.7	21.8
0800-0900	204	59	0.00	145	0	24.2	23.4
0900-1000	218	73	0.04	140	5	24.7	24.0
1000-1100	527	167	0.17	309	51	25.5	25.5
1100-1200	669	167	0.35	373	129	26.4	26.5
1200-1300	567	84	1.28	212	271	28.9	27.8
1300-1400	421	28	0.09	361	32	29.6	27.3

TABLE III ----Continued

mb	T°C.	mb	u M/sec.	u M/sec.	$\frac{u_{20M.}}{u_{1 M.}}$	dd		Cloud
20.5	0.02	-0.24	3.39	5.15	1.52	S	1	Ci
21.0	0.01	-0.20	2.81	4.53	1.62	S	0	Ci
22.1	0.07	-0.19	1.43	2.94	2.05	S	3	Ci
22.7	0.08	-0.13	1.03	3.17	2.21	S	1	Ci
22.8	0.24	-0.14	1.01	8.33	3.19	SSE	1	Ci
21.6	0.35	-0.04	1.48	5.50	3.72	SSE	0	--
21.4	0.30	-0.10	.24	2.27	9.42	SSE	0	--
21.2	----	-----	.41	2.41	5.91	SSE	0	--
19.0	----	-----	1.97	3.81	1.93	SSE	0	--
17.3	----	-----	1.00	3.68	1.51	SSE	0	--
----	----	-----	.88	2.73	3.08	SSE	0	--
17.5	----	-----	.58	2.24	4.80	SSE	0	--
17.6	----	-----	.50	2.29	4.61	SSE	5	Ac,Sc
17.6	----	-----	.41	2.23	5.40	SSE	9	Ac,Sc
17.5	----	-----	.85	2.87	3.32	SSW	6	Ac,Sc,Ci
17.6	0.12	-0.12	.39	2.02	5.10	SSW	9	Ac,Sc,Ci
18.4	-0.03	-0.18	.63	2.08	3.28	SW	9	Ac,Sc,Ci
19.3	-0.00	-0.09	.79	3.06	3.90	SSW	9	Ci
20.4	-0.02	-0.29	---	-----	----	SSW	9	Ci,Ac,Ad
21.1	-0.12	-0.44	---	-----	1.87	SW	6	Ci,Ac,Sc
21.8	-0.33	-0.60	1.21	2.03	1.62	SW	6	Ci
24.8	-0.08	-0.04	---	-----	----	SW	7	Ci,Ac,Cu
25.3	-0.10	-0.72	---	-----	----	SW	7	Ci,Ac,Cu

A7

TABLE IV

HEAT BUDGET OVER UNIVERSITY OF WISCONSIN
MARSH FARM CORNFIELD

Time	R_o	B_o		E	L	T_o°C.	T°C.
June 18							
1000-1100	0.886	01076	0.753	0.462	0.348	41	20.24
1100-1200	0.976	0.074	0.698	0.531	0.370	46.5	21.48
1200-1300	0.897	0.062	0.761	0.476	0.359	50.0	22.32
1300-1400	0.587	0.075	0.819	0.282	0.230	49.8	22.11
1400-1500	0.499	0.065	0.954	0.221	0.212	41.1	22.32
1500-1600	0.418	0.039	0.783	0.212	0.166	40.7	22.12
1600-1700	0.281	-0.0004	0.930	0.146	0.135	39.6	21.87
1700-1800	0.076	-0.053	0.716	0.075	0.054	31.3	21.38
1800-1900	-0.060	-0.058	0.522	-----	-----	24.0	20.44
1900-2000	-0.134	-0.076	-1.678	0.086	-0.144	18.4	16.04
2000-2100	-0.129	-0.066	-3.836	0.022	-0.085	14.7	14.44
2100-2200	-0.125	-0.065	-14.838	0.004	-0.064	13.1	13.99
2200-2300	-0.112	-0.053	-2.887	0.031	-0.090	12.0	12.43
2300-2400	-0.076	-0.051	-2.0	0.025	-0.050	12.1	-----
June 19							
0000-0100	-0.074	-0.074	-1.067	0.065	-0.65	13.5	14.03
0100-0200	-0.084	-0.063	-1.251	0.084	-0.105	13.6	13.69
0200-0300	-0.102	-0.057	-6.378	0.008	-0.053	11.8	11.79
0300-0400	-0.059	-0.028	-4.909	0.008	-0.039	11.4	12.01

TABLE IV ----Continued

mb	T°C.	mb	u M/sec.	u M/sec.	$\frac{u_{30M.}}{u_{1\ M.}}$	dd	Cloud	
11.93	20.24	-1.27						
11.67	21.48	-1.48				SW	1	St
11.42	22.32	-1.78				W	4	Ci,Cu
11.24	22.11	-1.30	3.4			NW	5	Ci
11.07	22.32	-0.74	5.7			NW	8	Ci
10.63	22.12	-0.86	6.1			NW	6	Ci
11.08	21.87	-0.78	8.2			NW	7	Ci
10.99	21.38	-0.78	10.1				2	Ci
11.77	20.44	-0.32	11.4				0	
13.26	16.04	-0.18	1.3				0	
12.39	14.44	-0.17	1.6				0	
11.76	13.99	-0.05	1.5				0	
11.46	12.43	0.30	1.8				0	
-----	-----	-----	1.1				7	Ci
12.31	14.03	-0.33	0.7				-	
12.68	13.69	-0.21	---				5	St
11.63	11.79	0.06	1.1				1	St
11.92	12.01	-0.07	0.6			NW	9	Ac

TABLE V

HEAT BUDGET OVER UNIVERSITY OF WISCONSIN
MARSH FARM CORNFIELD

Time	R_o	B_o			E	L	T°C.
May 28							
0430-0530	-0.057	------	-1.93	4.00	-----	------	8.60
0530-0630	0.058	0.012	0.09	-0.46	0.085	-0.039	9.85
0630-0730	0.243	0.079	0.46	0.33	0.123	0.041	10.53
0730-0830	0.498	0.093	0.20	0.24	0.327	0.078	11.56
0830-0930	0.701	0.097	0.27	0.25	0.483	0.121	12.22
0930-1030	0.641	0.080	0.23	0.23	0.456	0.105	12.60
1030-1130	0.863	0.039	0.22	0.31	0.629	0.195	13.76
1130-1230	0.751	0.020	0.29	0.25	0.584	0.146	13.64
1230-1330	0.601	-0.001	0.23	0.30	0.463	0.139	13.37
1330-1430	0.583	-0.029	0.22	0.28	0.478	0.134	13.23
1430-1530	0.321	-0.050	0.19	0.35	0.274	0.096	12.26
1530-1630	0.318	-0.068	0.24	0.22	0.316	0.070	10.92
1815-1830	-0.011	-0.065	-0.18	0.21	0.045	0.009	9.79
1830-1930	-0.032	-0.075	-0.27	-0.50	0.086	-0.043	9.65
1930-2030	-0.047	-0.062	-0.35	-0.78	0.068	-0.053	9.11
2030-2130	-0.039	-0.058	-0.52	-0.49	0.037	-0.018	8.86
2130-2230	-0.048	-0.056	-0.45	-0.65	0.022	-0.015	8.51
2240-2335	-0.127	-0.088	-0.82	-2.50	0.026	-0.065	7.42
2341-0030	-0.121	-0.102	-1.82	-5.00	0.005	-0.024	6.19
May 29							
0030-0130	-0.126	-0.096	-3.30	-5.36	0.007	-0.037	5.18
0130-0230	-0.127	-0.073	-2.05	5.36	-0.009	-0.045	5.40
0230-0330	-0.123	-0.087	-3.20	11.32	-0.003	-0.033	4.47
0330-0430	-0.118	-0.068	5.04	4.24	-0.009	-0.041	3.05
0430-0530	-0.064	-0.025	----	2.30	-0.012	-0.027	4.88
0530-0630	0.119	0.046	0.26	-0.27	0.100	-0.027	7.68
0630-0730	0.344	0.077	0.40	0.61	0.166	0.101	9.53
0730-0830	0.633	0.130	0.37	0.66	0.304	0.199	12.75
0830-0930	0.819	0.186	0.40	0.58	0.400	0.233	14.12
0930-1030	0.941	0.244	----	0.74	0.400	0.297	15.19
1030-1130	0.017	0.227	0.61	0.90	0.415	0.374	17.08
1130-1200	1.053	0.197	0.65	0.77	0.483	0.372	17.67
1200-1300	1.025	0.142	0.80	0.93	0.457	0.425	18.22
1300-1400	0.993	0.086	0.73	0.88	0.482	0.424	19.09
1400-1500	0.594	-0.014	0.60	1.04	0.298	0.309	19.14
1500-1600	0.354	-0.066	0.60	0.78	0.235	0.184	18.63
1600-1700	0.200	-0.082	0.56	0.76	0.160	0.121	18.45
1700-1800	0.148	-0.101	0.58	3.87	0.051	0.197	18.45
1800-1900	-0.032	-0.144	-0.01	-0.09	0.123	-0.011	16.46
1900-2000	-0.054	-0.085	-0.73	-0.23	0.040	-0.009	15.15

TABLE V ----Continued

mb	T°C.	mb	u M/sec.	u M/sec. $\frac{u_{30M.}}{u_{1\ M.}}$	dd		Cloud
7.66	0.06	0.01	---	---	---	-	--
8.28	0.22	-0.30	---	---	---	-	--
8.00	-0.18	-0.36	---	---	WNW	0	Fe
7.92	-0.26	-0.71	6.2	2.8	WNW	1	Fe
8.22	-0.36	-0.92	6.9	3.8	WNW	2	Cu
8.46	-0.33	-0.92	6.9	3.8	WNW	7	Cu
9.43	-0.53	-1.11	7.0	4.6	WNW	7	Cu
9.00	-0.46	-1.18	7.6	4.9	WNW	9	Cu
8.81	-0.49	-1.04	8.1	5.4	WNW	8	Cu
8.75	-0.36	-0.81	6.7	4.8	WNW	8	Cu
8.16	-0.38	-0.71	6.6	5.5	NW	9	Cu
7.82	-0,23	-0.65	6.5	5.4	NW	4	Cu
7.86	-0.15	0.45	---	---	NNW	-	--
7.24	0.20	-0.26	3.6	2.8	NNW	9	Cu
6.85	0.33	-0.28	3.4	3.2	NW	10	Cu
6.71	0.22	-0.29	3.2	2.4	NW	10	Cu
6.94	0.21	-0.21	2.9	---	NW	10	Cu
6.24	0.25	-0.07	2.8	---	NW	0	--
6.26	0.45	-0.07	2.6	---	NNW	0	--
6.31	0.67	-0.08	---	2.4		0	--
6.43	0.67	0.08	---	2.8		0	--
6.40	0.85	0.05	---	2.7		0	--
6.27	0.85	0.12	---	2.2		0	--
6.90	0.36	0.13	---	2.7		0	--
7.90	0.05	-0.12	2.2	3.2		0	--
8.53	-0.43	-0.45	1.9	2.8		0	--
8.57	-0.61	-0.60	1.5	2.2		0	--
8.03	-0.93	-1.03	---	3.7		0	--
----	-0.83	----	---	3.8		0	--
9.01	-1.08	-0.79	1.9	1.7		1	Ci
9.24	-1.17	-0.97	2.3	1.9		1	CiCu
8.79	-1.28	-0.88	1.7	2.3		3	CiCu
8.51	-1.59	-1.15	2.1	2.4		7	CiCu
8.25	-1.45	-0.89	2.5	2.8		8	CiCu
8.04	-1.12	-0.91	2.9	5.9		9	Ci
8.31	-0.61	-0.52	2.6	3.1		7	Ci
8.62	-0.29	-0.05	2.7	3.3		8	Ci
8.84	0.07	-0.49	1.7	2.3		8	Ci
9.44	0.13	-0.37	---	2.4		-	--

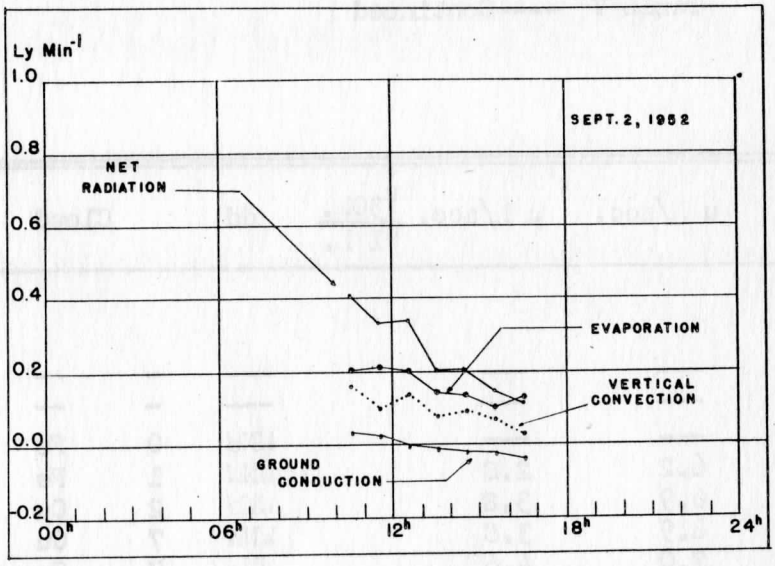

Figure 5

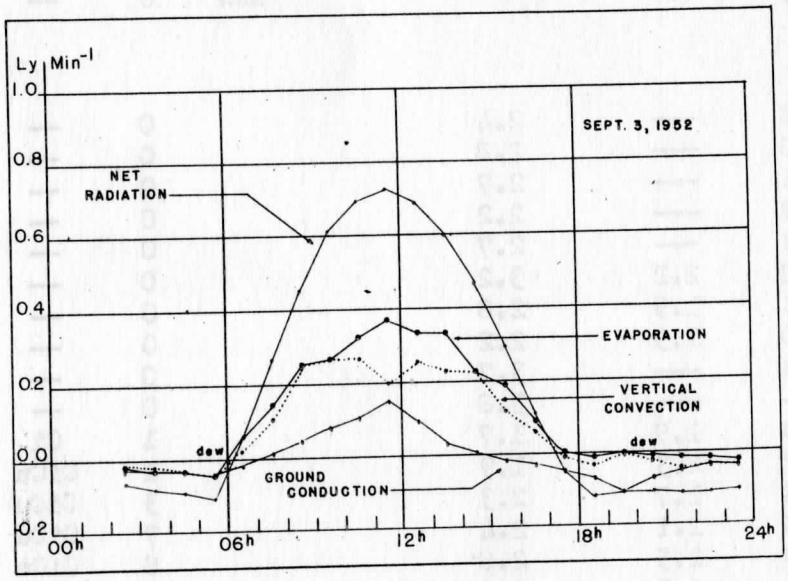

Figure 6

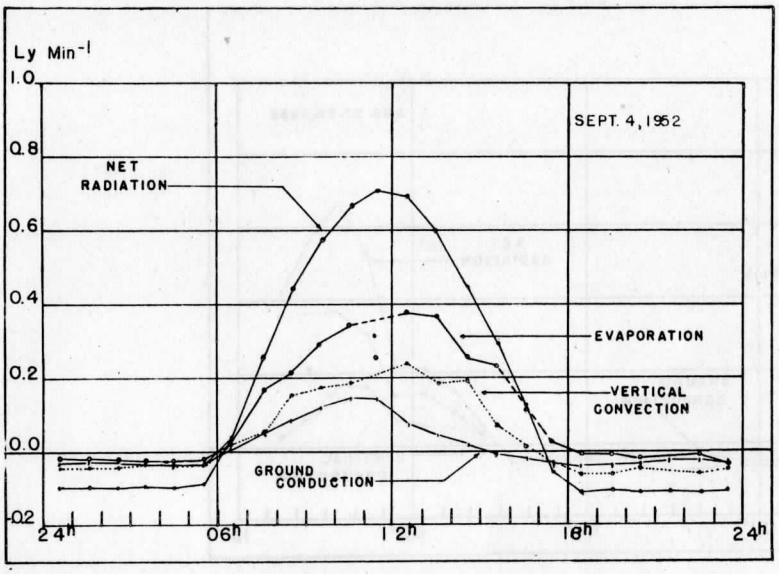

Figure 7

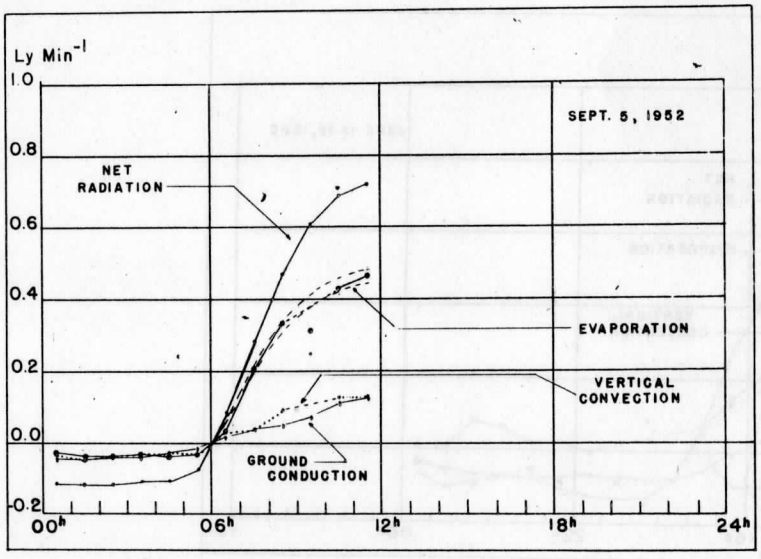

Figure 8

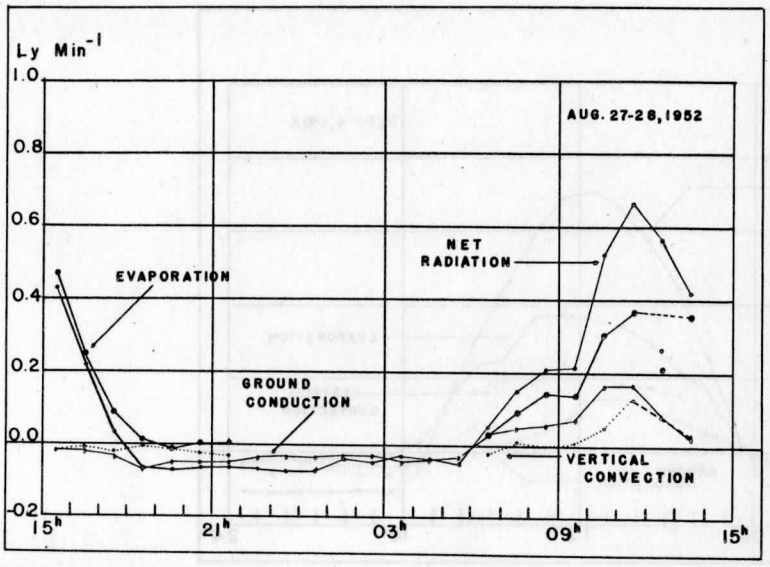

Figure 9

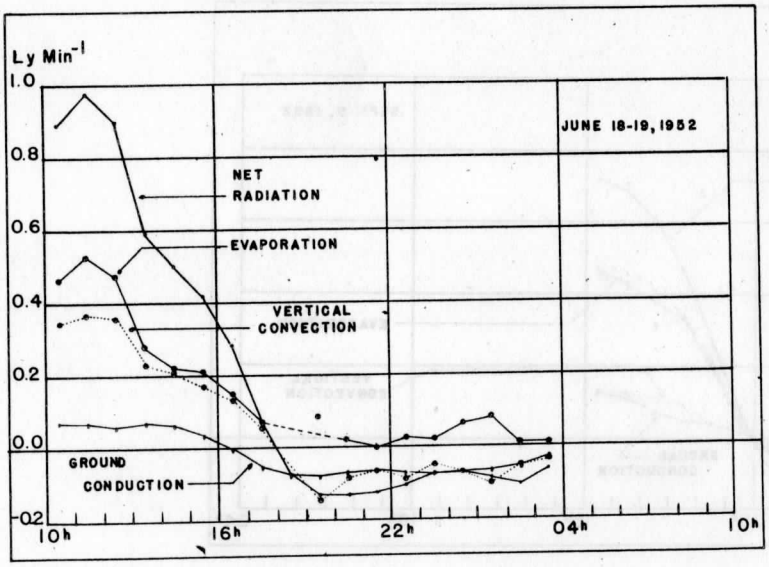

Figure 10

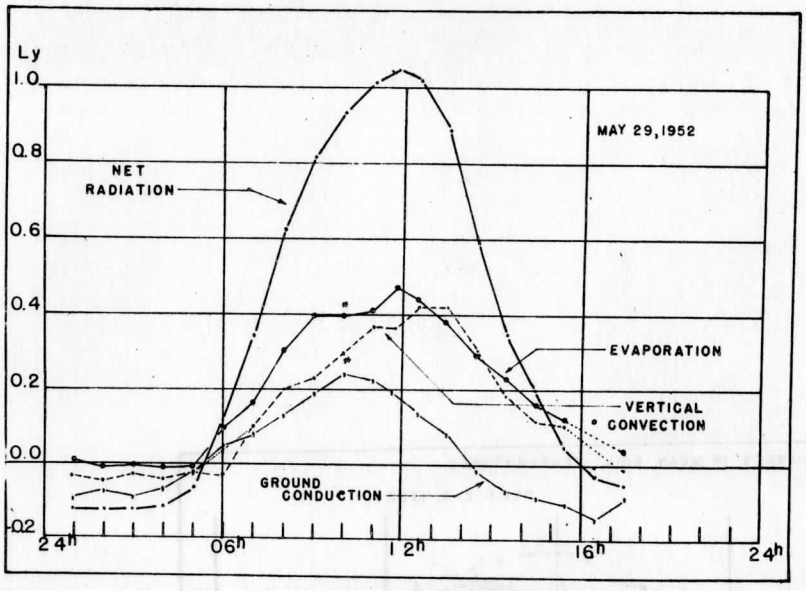

Figure 11

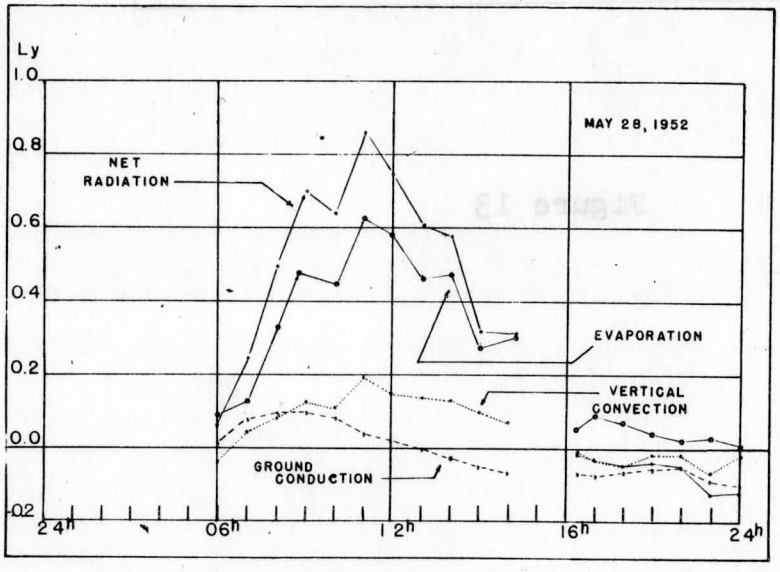

Figure 12

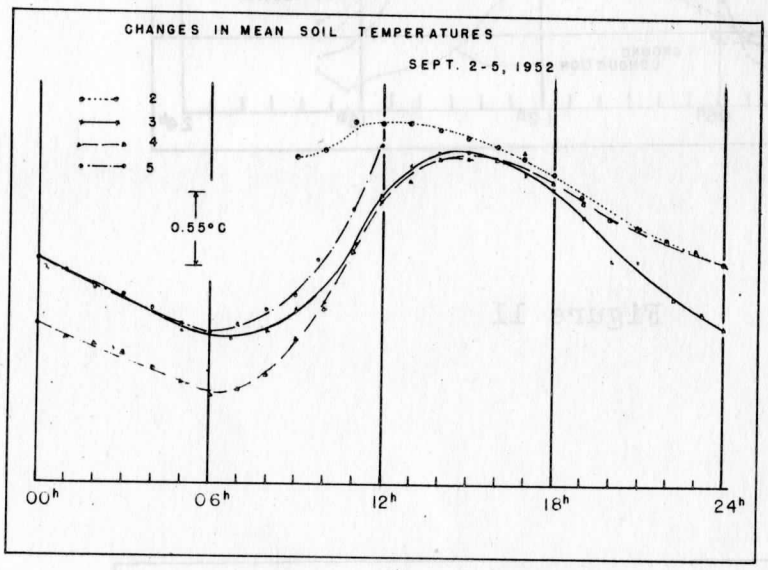
CHANGES IN MEAN SOIL TEMPERATURES
SEPT. 2-5, 1952
2
3
4
5
0.55°C
00h
06h
12h
18h
24h

Figure 13

REFERENCES

Albrecht, F., 1943 Meteor. Zeitschrift 60, p 44.

Businger, J. A., 1954 Med. Verh. K. Ned. Meteor. Inst., No. 61, 78 p.

Deacon, E. L., 1949 J. r. Meteor. Soc. 76, p 479.

Erbel, H., 1942 Met. Zeitschr 59, p 250.

Geiger, R., 1950 "Climate near the Ground," (Harvard University Press.)

Gerhardt, F. R., and Gordon, W. E., 1948 Jour. Meteor. 5 p 119.

v. d. Held, E. F. M., 1947 Standaarddictaat, "Gelykvormigheidsleer," Urrecht.

Lettau, H. H., 1949 Air Force Cambridge Research Lab. Geophys. Paper No. 1

Lokken, S. T., 1950 M. S. Thesis Univ. Wisc.

Martinelli, C. C., et. al., NACA Advance Res. Rpt. 4H09 (Aug. 1944).

Pasquill, F., 1949 Proc. Roy. Soc. 198 Ser. A, p 136.

Priestley, C. H. B., and Swinbank, W. C., 1947 Proc. Roy. Soc. 189 Ser. A. p 543.

Rider, N. E., 1954 Phil. Trans. Roy. Soc. A 246 p481

Rider, N. E., and Robinson, G. D., 1951 Quart. J. r. Meteor. Soc. 77 p 375

Shannon, C. E., 1949 Proc. Inst. Radio Eng. 37 p 10.

Spilhaus, A. F., 1936 Trans. Roy. Soc. So. Africa, 24 p 185.

Suomi, V. E., Franssila, M., and Islitzer, N. F., 1953 Sic. Rept. No. Contract AF19(122) -461, Dept. Meteor., Univ. of Wisconsin.

Swinbank, W. C., 1951 Jour. Meteor. 8 p 141.

Vehrencamp, J. E., 1953 Trans. Amer. Geophys. Union 34 p 22.

POWER SPECTRUM OF SONIC ANEMOMETER WIND AND SONIC TEMPERATURE MEASUREMENTS

I. Introduction:

In a number of problems concerning turbulent motion in the boundary layer near the earth's surface, it is especially helpful to be able to resolve the wind V, into its three components. Ordinarily u is taken in the direction of the mean wind, v and w are taken normal to the mean wind, the former being horizontal and the latter vertical. In such a co-ordinate system it is clear the v and w components can take on either sign. A suitable anemometer must, therefore, be able to measure the wind component through zero to negative values.

Of particular interest to studies of turbulent motion is the distribution of eddying energy with respect to the scale of the motion. If we assume that the time a turbulent element takes to pass the point of observation is much shorter than its lifetime, then the scale is related to the mean wind by the expression

$$L = \frac{\bar{V}}{n}$$

where $\bar{V}$ is the mean wind and n is the frequency of the wind fluctuation. Insight into the problem of determining where in the scale range the eddying energy is generated and where it is dissipated is considerably enhanced by presenting the wind data in the form of its power spectrum.

The first purpose of this paper is to describe a sonic

anemometer-thermometer which can resolve the wind into components with high accuracy. The anemometer makes use of the fact that sound traveling with the wind goes faster than sound traveling against the wind. The sonic anemometer's output is linear with wind velocity over a wide range on each side of zero. The sonic thermometer makes use of the fact that the average velocity of sound with and against the wind is proportional to the square root of the absolute temperature. A second purpose is to describe a means for obtaining a record of the wind component from the anemometer in a form that lends itself to analog methods of power spectrum analysis. Finally, the details of several analog methods of power spectrum analysis and some sample analyses are given.

II. Sonic Anemometer Theory:

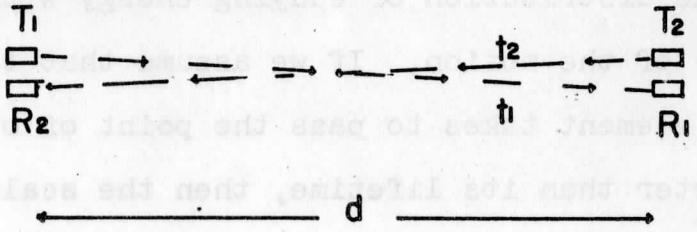

fig.1

Consider the array shown in Figure 1, where T_1 and T_2 are sound pulse generators and R_1 and R_2 are the respective detectors, separated a distance d, from the transmitters. Receiver R_1 receives the sound pulse from T_1 and so on.

It is easy to show that the difference in transit time for the sound pulses traveling in opposite directions is given by the expression

$$\Delta t = \frac{2 d V_a}{V^2 - C^2} \qquad (1)$$

where d is the distance between transmitter and receiver, V_a is the line average component of wind parallel to the direction d, of the array, C is the line average velocity of sound along the path in the medium and V is the <u>total</u> wind. In obtaining this expression, Blochinzev (1946), we use the same relations that apply in geometrical optics, i.e., that the inhomogenities in the medium are larger than the wave length of sound. In addition we assume that the sound traveling in each direction follows the same path, this point will be elaborated upon later.

Ordinarily $C^2 \gg V^2$ so we may write with good accuracy

$$\Delta t, = \frac{2 d V_a}{C^2} \qquad (2)$$

At ordinary temperatures if the total wind is less than 50 mph the error resulting by dropping the V^2 term is less than .5%. An elementary physics text book will show that

$$C^2 = \gamma R T = \gamma \frac{p}{\rho} \qquad (3)$$

γ is the ratio of specific heats of air, R is the specific

gas constant and the other terms have their usual meanings.

It is easy to show that in atmosphere near the surface

$$\frac{\delta T}{T} \simeq 3 \times 10^{-3} \; ; \; \frac{\delta \rho}{\rho} \simeq -3 \times 10^{-3} \text{ and } \frac{\delta p}{p} \simeq 10^{-5}$$

where δT, $\delta \rho$ and δp are the short time fluctuations of temperature, density and pressure respectively. Pressure fluctuations are two orders of magnitude less than density fluctuations. We can substitute (3) into (2) and assume p constant with an error of less than 1% and obtain

$$\Delta t_1 = \frac{2 \alpha \rho V_a}{\gamma p} = K \rho V_a$$

Thus the difference in transit time is equal to the mass transport accurate to better than 1%.

III. Sonic Anemometer

Credit for the first sonic anemometer should go to Carrier and Carlson (1944) who described a true air speed indicator for use on a blimp. Their instrument only partially completed, measured the difference in transit time in terms of phase difference between signals received at two microphones, one located up wind and another down wind from a continuous sound source. They also described

a servo controlled computer which would convert the phase difference to a wind velocity (air speed in their case) but they did not have the opportunity to complete the instrument. Suomi (1946) described a pulse type sonic anemometer where small spark discharges were used to generage the sound pulses. This instrument was simply two sonic thermometers (Suomi and Barrett (1949, placed in opposition.

The transit time difference can be obtained with a number of instrument arrangements. Corby (1950) has described an anemometer using a single sound source. Four microphones were placed equidistant at the four cardinal points of the compass. Schotland (1955) describes the theory and circuit of an almost identical instrument.

In order to obtain an instrument useful for studies of turbulent motion, it is essential that the sound generating and sensing heads be as small as possible, otherwise the turbulent wakes from these objects will generate enough turbulence to obscure the phenomenon under study. Also, the theory developed in the previous section assumes that the sound waves travel over the same path. Those sonic anemometers which have a single sound source and sensors up and downwind from it do not meet this requirements.

When the two sound paths are not identical we must

account for errors in the wind velocity caused by differences in the velocity of sound C, in the seperate paths. These differences in sound velocity are due to inhomogeneities in the temperature field. Gerhardt and Crain (1950) have measurements of the temperature difference observed between two rapid response thermistors as a function of distance separating them. The RMS temperature differences extracted from Gerhardt and Crain's paper are given in Figure 2.

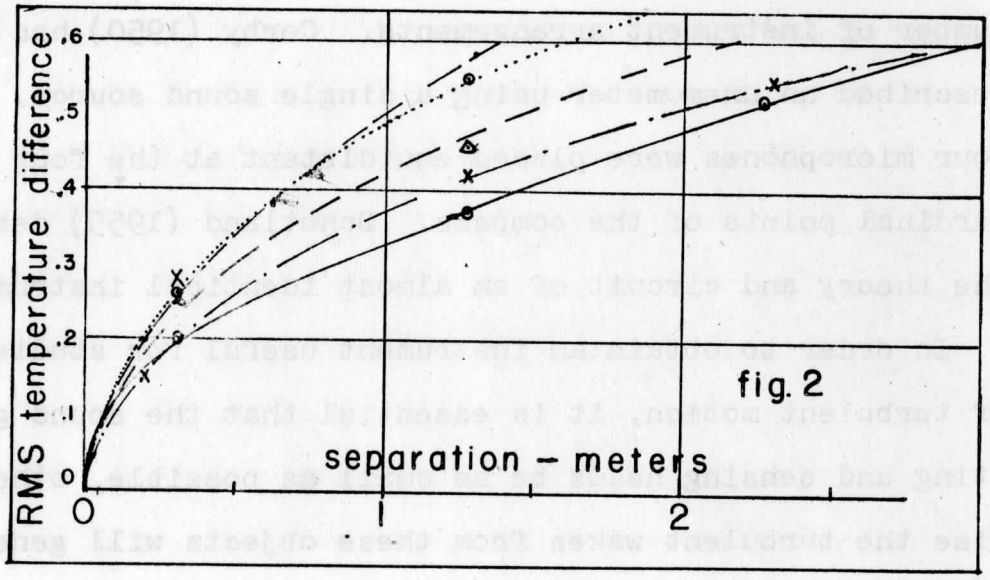

fig. 2

Those sonic anemometers which have a single sound source and microphones upwind and downwind will be subject to a sizable error due to temperature inhomogenity. If the two sound paths are 1 meter apart the RMS wind velocity error using Gerhardt and Crain's data will be 0.4 meters/sec. Such an error is intolerable when making

heat flux measurements since there will be a hidden correlation between temperature and vertical wind.

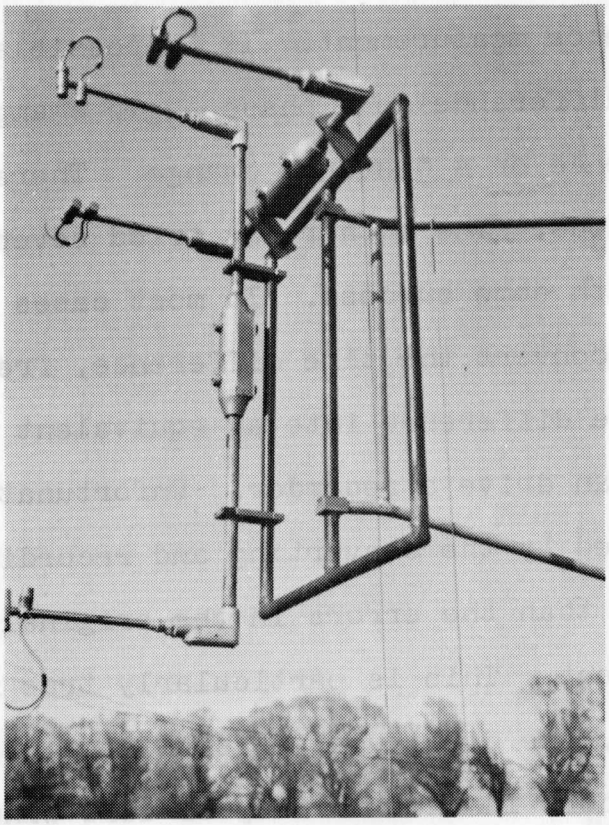

Figure 3

Figure 3 shows the acoustic array for a 1 meter path length pulse type sonic anemometer. The transmitting and receiving heads are located 1.5 cm from each other. Since the sound paths cross, the effective spacing is only .75 cm. The RMS temperature error using

Gerhardt and Crain's data is only 0.03 degree. This is equivalent to 0.02 M/sec wind error.

IV. Delay type sonic anemometer:

The output data from the sonic anemometer is basically a time difference measurement. It is possible to measure this time difference as a phase angle change, a frequency difference or a distance change. There are no doubt other methods. The author has tried several of these methods with some success. In most cases an attempt is made to convert the time difference, frequency difference, or phase difference into an equivalent electrical current which can drive a recorder. Unfortunately the errors introduced by the converting and recording systems are greater than the errors in the original time difference measurement. This is particularly true near zero wind. In fact, the difficulties associated with obtaining a good record in the vicinity of zero wind were so vexing that the whole sonic anemometer development was almost abandoned. Fortunately, the solution to this difficulty turns out to be extremely simple. The problem of obtaining good accuracy and stability arises from the fact that the difference in transit time at low velocities is very small. Therefore, in addition to sensing which sound pulse arrives first, the electronic circuits

must turn on and off very rapidly. In order to detect a wind change of .1 m/sec it is necessary to measure the time difference to 1 μ sec. This is easy to do at radar frequencies and even radio frequencies, but it is difficult to do at ordinary audio frequencies. There can be an <u>apparent</u> change in arrival time due to changes in the signal to noise ratio of the received signal. The problem of which sound pulse arrives first is easily solved by sending one pulse first then the other a short time later. The timing accuracy of the received pulse is improved by using super sonic frequencies. We now use short bursts of 80 kilocycle sound energy. T_1 is fired 100-200 μ sec before T_2 depending on the range of wind velocities being measured.

Figure 4 shows a block diagram of the delay sonic anemometer system. The time delay D_1 is chosen so that the signals will always arrive at R_1 first for the range of wind velocities expected.

Since R_1 is always received first this signal can be used to trigger the (X axis) sweep on a timing device such as a synschroscope. The reception of R_2 can be used to displace the sweep (Y axis) or to blank it (Z axis). If the duration of the sweep is just twice the delay time the "pip" or blanking will occur in the middle of

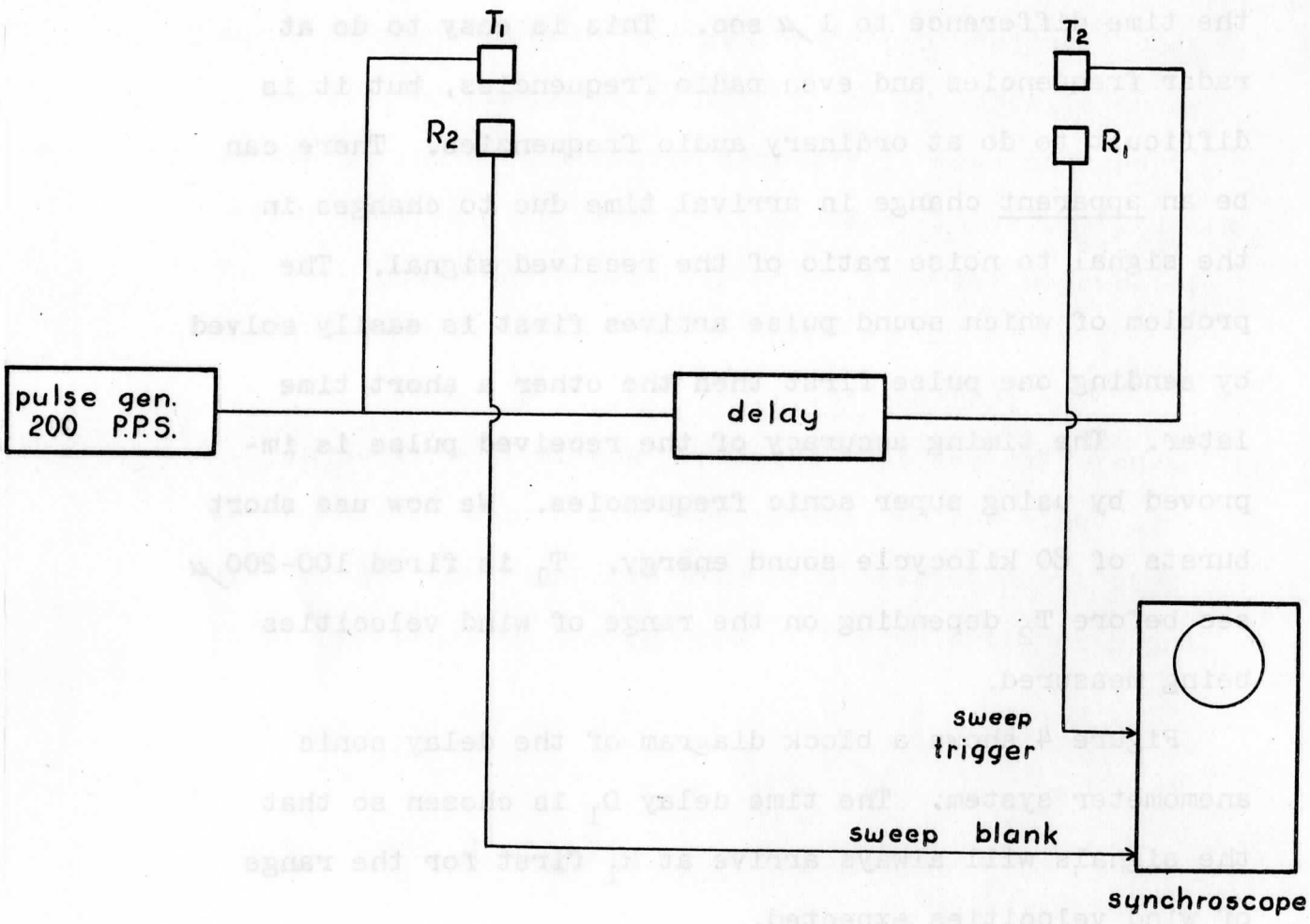
T1
T2
R2
R1
pulse gen.
200 P.P.S.
delay
sweep
trigger
sweep blank
synchroscope

Figure 4

the screen. The true zero wind point is easily established by simply measuring the duration of the delay D_1, directly.

V. Method of Recording:

Evidently, it is possible to convert the transit time difference and fixed delay into a current suitable for recording. However, all of the problems attendant to DC amplification will be raised. The wind information presented on the synchroscope is a line of light whose length changes depending on the direction and magnitude of the wind. If the wind has a high positive value it is long, if it has a high negative value, it is short. If the wind is zero it is 1/2 full scale.

The variable length line of light is photographed with a 35 mm camera whose film is advanced at a constant rate normal to the image of the line of light. The shutter remains open for the entire length of a run. The film need be advanced only fast enough to prevent overlap of individual scope sweeps. Film speeds of only 3 - 6" per minute give a very satisfactory record. The record appears much the same as the variable area sound track used for motion picture recording. A sample record is shown in Figure 5.

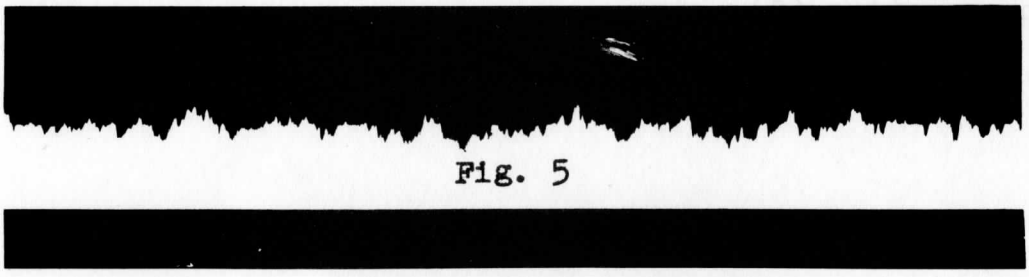

Fig. 5

The time scale calibration on each record is obtained with a fixed frequency oscillator which places timing marks on the Z axis of the synchroscope. Proper choice of oscillator frequency as a function of acoustic array length yields a calibration directly in mass transport units, or if a mean density is assumed, in velocity units. The zero position is established by a direct measure of the delay D_1.

VI. Combination Sonic Thermometer-Anemometer:

In Section II it was mentioned that the difference in transit time Δt, was proportional to the wind. In like manner the roundtrip time or average transit time is proportional to the inverse of the velocity of sound.

$$t_1 + t_2 = \frac{2dC}{C^2 - V^2} \qquad (4)$$

since $C^2 \gg V^2$

$$t_1 + t_2 = \frac{2d}{C} \qquad (5)$$

recalling that $C^2 = \gamma R T$ we have

$$t_1 + t_2 = \text{const.} \frac{1}{\sqrt{T}} \qquad (6)$$

Suomi and Barrett (1949, discuss the assumptions underlying equation (5).

They show that the sonic temperature T_s is

$$T_s = T\left(1 + 0.319\,\frac{e}{p}\right) \qquad (7)$$

where T is the air temperature, e the vapor pressure and p the atmospheric pressure. This expression is very similar to the meteorological quantity, the virtual temperature, which (see Holmboe (1949)) can be defined as

$$T^* = T\left(1 + 0.379\,\frac{e}{p}\right) \qquad (8)$$

At a true air temperature of 30° and a 30% relative humidity the sonic temperature is approximately 31° C. Since in turbulent studies we are mainly interested in temperature fluctuations, we can say

$$T'_{air} \approx T'_{sonic}$$

It is important to note that the temperature is averaged over the same path as the wind, therefore, for all practical purposes, wind and temperature are obtained from the same air sample at the same time.

VII. Scheme for Obtaining Temperature and Wind:

If the oscillator in Figure 3 were triggered by the reception of the R_1, we have a simple basis for measuring the total roundtrip time as illustrated in the time

diagram shown in Figure 6.

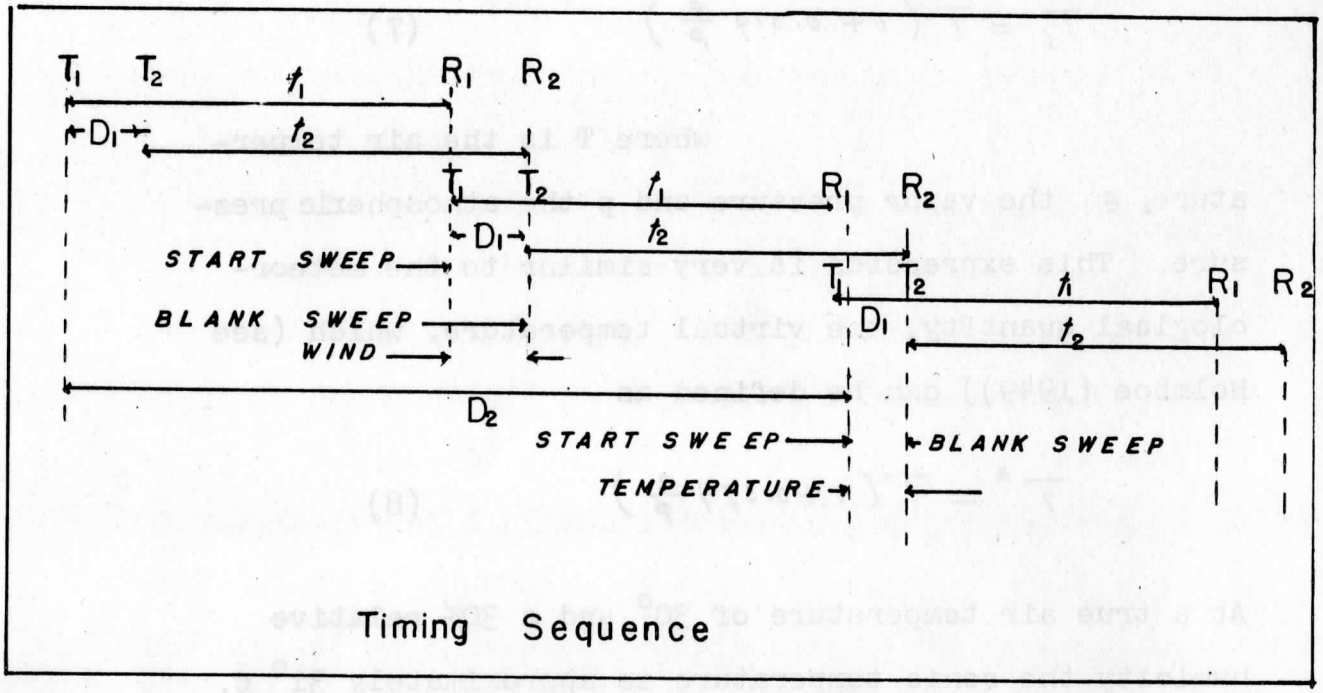

Figure 6

The total time to the reception of a signal at R_2 of alternate pulses is

$$D_1 + t_1 + t_2 + D_2$$

or

$$2D_1 + t_1 + t_2$$

If a very long delay D_2 is triggered at the time of T_1, and the scope sweep is triggered at the end of the long delay, the synchroscope will indicate the difference between D_2 and the roundtrip time, or

$$D_2 - (2D_1 + t_1 + t_2) = D - (t_1 + t_2)$$

where $D = D_2 - 2D_1$

but

$$t_1 + t_2 = \frac{2d}{C} = 2d(\gamma R T)^{-\frac{1}{2}} \qquad (9)$$

Expressing T as $T_o + T'$ and expanding (9) into 2 terms of the binomial series and subtracting D from each side, we have

$$t_1 + t_2 - D = 2\alpha(\gamma R)^{-\frac{1}{2}}\left(T_o^{-\frac{1}{2}} - \tfrac{1}{2}\frac{T'}{T^{3/2}}\right) - D$$

Since the value of D the total net fixed time delay is arbitrary, we set it equal to

$$2\alpha(\gamma R T_o)^{-\frac{1}{2}}$$

the scope trace Δt_2 is

$$t_1 + t_2 - D = -\alpha(\gamma R)^{-\frac{1}{2}}\frac{T'}{T^{3/2}}$$

Since $T_o \gg T'$ and, in addition, is very nearly constant, we can write to good accuracy

$$\Delta t_2 = \text{Constant} \cdot T'$$

VIII. Variance Spectrum Analysis:

The large amount of temperature or wind information available from the sonic anemometer on the variable area record film, will be much more useful if it is summarized into a more convenient form. The wind or temperature record represents a time series characterized by large numbers of small oscillations with a quasi-continuous

distribution of periods. While this time series can be summarized into well known statistical parameters, such as the mean, the variance, the frequency distribution and so on, the data is considerably more revealing if the variance is available as a function of frequency. In the case of a single variable this variance spectrum is often called the power spectrum. In other cases we are interested in a time series which results from the product of two variables. In the case of vertical heat flux this product would involve the vertical wind component and the temperature. Here we are interested in the cospectrum which is the variance of the product as a function of frequency. In still other cases where two variables are nearly independent the cospectrum may be low or zero over a wide range of frequencies. Under these conditions it is helpful to obtain the variance of the product when one of the variables is shifted in time corresponding to a 90° phase shift for that frequency. This product as a function of frequency is called the quadrature spectrum. In order to obtain any of these spectra one must have a means of separating from the total for all frequencies the energy (or product) that lies in the band from n to $n+\Delta n$, where n has values covering the whole range of frequencies. This

can be done using the mathematical filter developed by Wiener and outlined by Tukey (1949) if individual observations are available, or it can be done with an electrical or mechanical filter if electrical analogs of the original data are available.

The mathematical filter method is based on the theorem that the Fourier cosine transform of the auto correlation function (or cross correlation function) is essentially equal to the spectrum of the original series. Three calculations must be performed in order to obtain the spectrum.

1. Obtain the auto or cross correlation function. Obtain mean lagged products $\sum_{i=1}^{m} f_i(t) f(t+\tau)$ formed from the variable $f(t)$ and the same variable at time τ later for a number of values of τ. The number of lags m, will correspond to the number of data points in the fixed spectrum however, if m is large the numerical work is enormous. When the lagged products are from the same variable, we obtain the auto correlation

$$\phi_{ij}(\tau) = \lim_{T\to\infty} \frac{1}{T} \int_0^T f_i(t) f_i(t+\tau)\, dt \qquad (10)$$

When the lagged products are formed from two variables,

we obtain the cross correlation function

$$\psi_{ij}(\tau) = \lim_{T\to\infty} \frac{1}{T}\int_0^T f_i(t)\, g_i(t+\tau)\, dt \qquad (11)$$

2. Obtain Fourier cosine transform of (10) for the power spectrum and (11) for the cospectrum.

3. Making a moving average correction to the results of step 2. This amounts to "sharpening" the filter. The mathematical filter has the advantage that the spectrum obtained is smooth and thanks to Tukey, the reliability of the results is known. Panofsky and McCormick (1954), Griffith (1955), Cramer (1954) and others have used this technique to wind and temperature observations.

If the power spectrum is to be obtained with an electrical or mechanical filter it is first necessary to raise the frequency of the raw data to a much higher value with some scheme for time multiplication. Frequencies in the range from a few cycles per hour up to a few cycles per second are conveniently raised to the audio frequency range (10 cps-20KC) by splicing the record (magnetic tape, film etc.) into a loop so that it can be played back at high speed. Deacon (1949) used a fixed frequency mechanical filter in the form of a vibration galvanometer and changed the speed of the play back equipment to obtain the power spectrum of ocean waves. Pierson (1952)

obtained the power spectrum of ocean waves in a similar manner. Staake (1955) used a magnetic tape play back at a fixed speed and obtained the power spectrum using a commercially available Hewlett Packard audio frequency harmonic analyser. The output of the analyser is simply the sum of the frequencies passed by the filter. If this signal is squared and averaged over one tape loop as a function of frequency, one obtains the power spectrum.

IX. Band Saw Film Recorder:

In our case a sturdy, well balanced, band saw was used as the basic mechanical unit for the play back recorder. The film loop was used in place of the band saw blade. The reading head consisted of an illuminated narrow light slit (.001 in.) backed up by a photo multiplier and amplifier. The wind data was then available as the voltage output of the photo multiplier amplifier. Linearity of the slip and amplifier was checked with a play back of a pure sine wave record of large amplitude. Distortion introduced by nonlinearity in illumination of the slit, photo multiplier response, and amplifier was less than 1% of the signal. The amplifier frequency response was compensated to be flat from 10 cps to 100 KC. Figure 7 shows a block diagram for a method obtaining the power spectrum using a Hewlett Packard Harmonic frequency analyser.

This instrument consists of an adjustable band width fixed frequency filter whose center frequency is about 20 KC. The instrument also contains an audio oscillator and balanced modulator arranged so that the desired signal can be heterodyned for insertion into the narrow band constant frequency 20 KC filter. Staake (1955) has described the use and limitations of the Hewlett Packard instrument in a similar application. The instrument, as it comes from the manufacturer has a linear detector which yields the amplitude spectrum. Since we are interested in the variance spectrum of the wind which is the signal power as a function of frequency, it was necessary to replace the linear detector with a squaring device, wide range linear detector and integrator.

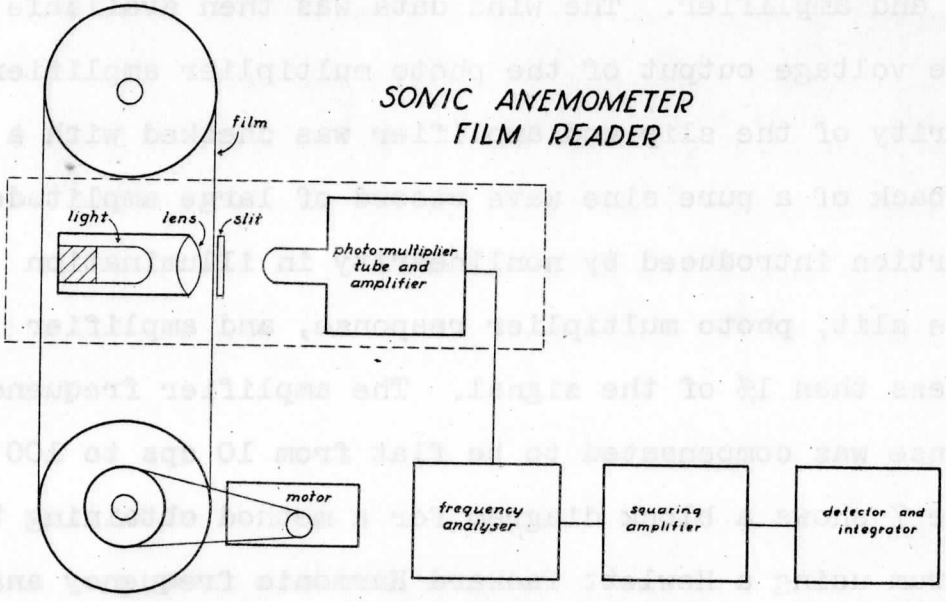

Figure 7

X. Cospectrum and Quadrature Spectrum Analyses:

It is possible to otbtain the cospectrum and the quadrature spectrum in a similar manner with the use of two frequency analysers.

The oscillator of frequency analyser 2 is disabled and its signal is replaced by the corresponding oscillator signal from analyser 1. The phase shift element between the two analysers is used to obtain the quadrature spectrum.

XI. Analog Variance and Covariance Spectrum Analyses Using Auto and Cross Correlation:

If one has available a high quality analog multiplier, a time delay device, and an integrator, one can obtain the auto correlation function or cross correlation function using analog methods. A high speed correlator of this type has been developed by Bell and Rideout (1954). The correlator will do the calculations of Step 1, of the mathematical filter computation procedure outlined earlier. The remaining steps involving a much smaller number of data can then be carried out with a desk calculator or automatic digital computor.

When this system is employed, one has then taken the advantage of the analog system (its high speed) and also the advantage of the mathematical filter (its smooth spectrum and a knowledge of the errors) without the labor of long computation. A comparison of the power spectrum of the

vertical wind obtained with the frequency analyser and the analog autocorrelation technique is shown in Figure 8.

The author had the good fortune of having available the high speed analog correlator developed by Bell and Rideout (1954) at the University of Wisconsin. The correlator uses a lumped constant delay line to provide a time delay in 41 steps up to a maximum of 2080 micro seconds. A block diagram of the correlator is shown in Figure 9. The 2080 micro second maximum time delay is equivalent to an actual time delay of 20.8 seconds at a play back speed 10,000 times as fast as the original film speed. The time required to obtain the complete auto correlation function is less than a minute! The 41 values of mean lagged products given by the correlator are placed on IBM punch cards. A IBM 650 electronic calculator, programmed to compute the Fourier cosine transform and filter function corrections has the complete variance or cospectrum calculated in about 5 minutes! The power spectrum shown in Figure 8 was obtained this way.

With only a little more trouble and considerably less expense, one can obtain the time delays required for the auto correlation and cross calculation with the time

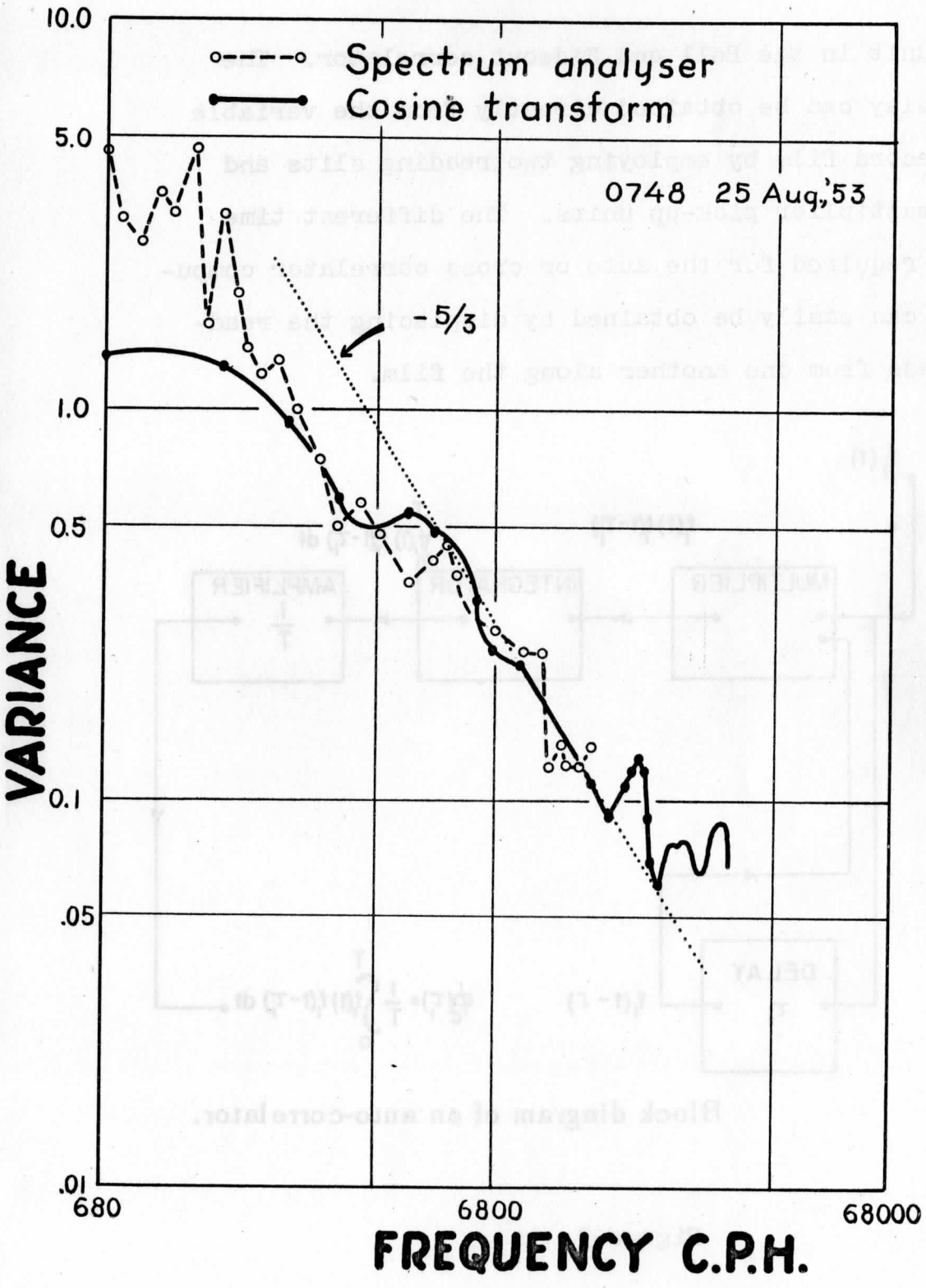
Spectrum analyser
Cosine transform
0748 25 Aug,'53
-5/3
10.0
5.0
1.0
0.5
0.1
.05
.01
VARIANCE
680
6800
68000
FREQUENCY C.P.H.

Figure 8

delay unit in the Bell and Rideout correlator. The time delay can be obtained directly from the variable area record film by employing two reading slits and photo multiplier pick-up units. The different time delays required for the auto or cross correlator computation can easily be obtained by displacing the reading heads from one another along the film.

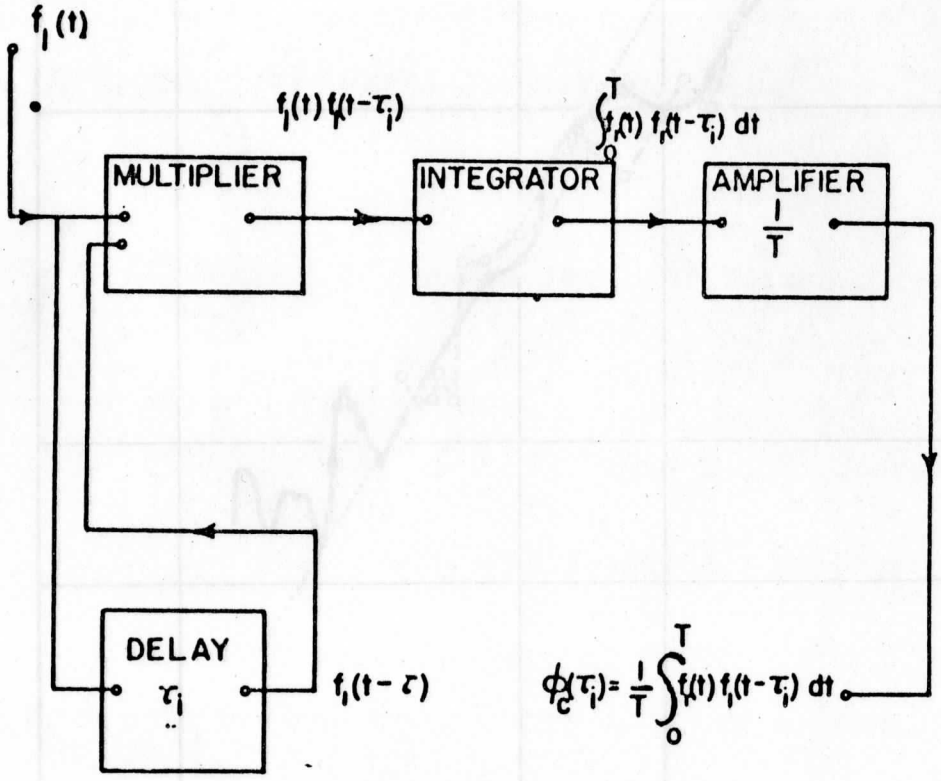

Block diagram of an auto-correlator.

Figure 9

XII. Conculsion:

We have described a sonic anemometer and thermometer of good accuracy and high speed. The instrument is not an experimental model, but has been used in the field under many operating conditions. Its physical characteristics are known very well i.e., it measures the line average component of mass transfer and the line average value of the virtual temperature. Its output can be available as a variable area film record, which lends itself to high speed playback and analog computation. Methods of power spectrum, cospectrum, and quadrature spectrum analysis using purely analog methods and a combination analog and digital methods are given. It would appear that measurements made and recorded with the equipment described will yield useful information on the structure of turbulence near the ground.

REFERENCES

Bell, H., and Rideout, V. C., IRE Transactions, Vol. EC-3, No. 2, 30 June 1954; see also U. of Wisconsin, Eng. Exp. Station, Reprint No. 252.

Blochintzev, 1946 Journal Acoust. Soc. of America, 18, p 332.

Carrier, and Carlson, 1944 NDRC Report, Craft Laboratory, Howard University.

Corby, R. E., 1950 Electronics 23,p 88.

Cramer, H. E., G. C. Gill, and Record, F. A., 1954 Final Report Contr. No. AF19(604)-145.

Deacon, G. E. R., 1949 Quart. Journal Roy. Met. Soc., 75, p 227.

Gerhardt, J. R., and Crain, C. M., 1950 Journal Met. 8, p 363.

Griffith, H. L., 1955 M.S. Thesis, Dept. of Meteor., Penn. State U.

Holmboe, J., et. al. 1949 "Dynamic Meteorology," John Wiley and Sons, Inc., New York.

Panofsky, H. A. and McCormick, R. A., 1954 Quart. Jour. Roy. Met. Soc. 80 p 546.

Pierson, W. J., and Marks, W., 1952 Trans. Am. Geophys. Union 33 p 834.

Schotland, R. M., 1955 Jour. Meteor. 12 p 386.

Staake, D. B., 1955 Johns Hopkins U., Appl. Phys. Lab., Rep. CM-833

Suomi, V. E., 1946 Final Report, Army Chemical Corps Contr., U. of Chicago, Dept. of Meteor.

Suomi, V. E., and Barrett, E., 1949 Jour. Meteor. 6, p 273.

Tukey, J. W., 1949 Symposium on Application of Auto-Correlation Analysis to Physical Problems, Woods Hole Ocean Inst., ONR, Washington D. C.,

Appendix:

CIRCUIT AND CONSTRUCTION DETAILS FOR SONIC ANEMOMETER THERMOMETER

by

V. E. Suomi, R. J. Parent and H. Miller

For purposes of discussion it is convenient to separate the sonic anemometer thermometer into the following main units:

(1) Transducer, Preamplifier and Pulse Generator Unit:

Two of these units or sound heads are needed to make up one axis of the acoustic array. There are two 80 KC ADP 45° Z cut piezo-electric crystals which act as a sound source and as a receiver for the opposite channel in each sound head. The preamplifier for the receiving crystal contains a voltage amplifier and a cathode follower amplifier so that the device will operate satisfactorily at the end of 500 ft. of cable. The pulse generator is a thyratron and pulse transformer circuit which when triggered from the main control chassis shocks the transmitting ADP crystal into oscillation at its resonant frequency. These units are shown in Figure 1 - 4, 7 and 8.

(2) Master Multivibrator:

This circuit is the main source of timing signals for the whole instrument. When the device is used only for wind measurements the multivibrator can be free running at a

frequency which on the low end is determined by the number of wind measurements per second that one wishes to make. The frequency is limited on the upper end by recovery time of the delay and sweep circuits. When the instrument is used as a combination anemometer-thermometer the master multivibrator must be operated at a frequency that will permit it to be synchronized from the signal from receiver No. 1.

(3) Short Time Delay Circuits:

Each delay circuit is a one shot multivibrator variable time delay unit. One circuit is used to obtain D_1 the wind delay mentioned in the previous section. Another similar circuit but of different time delay is used for what we have termed a "noise delay," or more properly, an interference eliminating delay. The purpose of the noise delay will be discussed further in a later paragraph. Each of these short time delay circuits must be variable and must have a relative timing stability, once set, to better than 1% of their pre-set values.

(4) Long Time Delay Circuit:

This circuit is used to obtain D_2 the "temperature delay," necessary for temperature information. It is not needed if only wind measurements are desired. The information needed for temperature measurements is the

difference of the roundtrip time $t_1 + t_2$ and the long delay, D_2. This difference measurement requires a much better timing stability than is possible from one shot multivibrators, phantastrons, or similar time delay circuits. The timing stability required is 1 part in 10^4, a value easily obtained in an oscillator. The circuit used is a pulsed oscillator and counting down circuit which makes use of Berkley preset counters. The time delay is varied by changing the integer of the divisor. Interpolation between each integer is obtained by changing the oscillator frequency over a 10% range.

(5) 80 KC Band Pass Amplifier, Detector and Level Selecting Channel:

Two identical channels are required. These together with a regulated power supply and the short time delay circuits make up the main anemometer chassis. Figure 5 is a block diagram of the complete sonic anemometer-thermometer showing the main circuits.

The circuit enclosed in the dotted box is the equipment that can be omitted if only an anemometer is desired. The circuit of Figure 5 presents both the temperature data and wind data on the same synchroscope. Two lines appear on the synchroscope screen, one for temperature, the other for wind. It is clear that two separate synchroscopes

can be used for wind and temperature data. This may offer an advantage in certain circumstances.

The block diagram of Figure 5 shows a noise delay circuit. This fixed delay was purposely left out of the earlier discussion of the sonic anemometer-thermometer theory to prevent confusion. This delay merely assures that each sound signal is received from the transmitter on the opposite end of the array before the adjacent transmitter is fired. It is clear that receiver No. 2 cannot distinguish the signal from transmitter No. 2, 1 meter or more away, from the signal from transmitter No. 1, only 1 centimeter away, despite any directional characteristics of the transducers if sound is received from each transmitter at the same time.

An understanding of the operation of the sonic anemometer-thermometer will be aided by a study of the oscillograms showing wave forms at various points in the circuit. We begin with the waveform on the plate of the master multivibrator shown as waveform 1 in Figure 6. After differentiation, polarity reversal, and power amplification in V_5, a spike shown in waveform 2 is available at a low impedance level to trigger transmitter No. 1 at the end of a 500 ft. cable. Meanwhile, the same signal (waveform 1) triggers a one shot delay multivibrator composed of the

tubes V_{3A} and V_4 to form the adjustable wind delay D_1, shown in waveform 3. The delayed signal is differentiated, polarity reversed and power amplified in V_2 to form another spike waveform 4, which triggers transmitter No. 2 at the end of the cable. Careful study of the timing marks will show that transmitter No. 2 is fired about 200 μ sec after transmitter No. 1. Up to this point no circuit operation depends on any <u>received</u> sound signals. A free running master multivibrator is satisfactory if only wind measurements are desired. Before discussing how the master multivibrator must be synchronized for temperature signals, it will be helpful to consider the circuit operation in the receivers. Waveforms 5 and 6 are the 80 KC amplified signals from R_1 before and after the detector diode 1N34. The smooth envelope signal is from T_1 on the opposite end of the array. The second larger and more variable signal is "noise" from T_2, located right next to R_1. Waveform 5 shows that a small amount of noise occurs at the same time as the spike for T_2. This probably represents acoustic coupling through the mount, since the velocity of sound in metals is much higher than that in air. Most of the noise, however, occurs a short time later via air coupling. Transit time t_1 is given by the distance separating the spike for transmitter 1 (waveform 2) and the smooth received pulse in waveforms 5 and 6.

Waveforms 7 and 8 are corresponding signals from receiver 2. Note that the smooth sound pulses from R_1 and R_2 in waveforms 5 and 7 are separated about the same distance as the wind delay D_2 shown in waveform 3. Actually the wind information is derived from the difference in these two times.

The rise times of the detected sound signals, waveforms 6 and 8, are far too slow for any accurate timing to be accomplished. The rise time is reduced in each case by amplification in a 6AK5 amplifier, V11 and V15, one for each channel, and then fed to a level selecting Schmitt circuit. The level selecting feature insures that the same portion of the waveform will be used in each signal. Since the level selector circuit is amplitude sensitive, provision for keyed automatic gain control V33, 34 and 35, for receiver 1 and 2, which can be used to hold the amplitude of the received pulses very nearly constant, can be accentuated by switch.

Wind data presented on a synchroscope will be available if the negative going portion of the waveform from the Schmitt circuit of receiver 1, is shaped as shown in waveform 10 and used to trigger the synchroscope sweep, and the corresponding signal from channel 2 is used to initiate waveform 11 for blanking (Z axis) of the sweep or to displace (Y axis) it.

A gated clamp on the grids of V11 and V15, eliminates any difficulty arising from noise signals if the noise signals occur after the desired sound signal. This will always be true for the received pulse from transmitter number 1, since the signal is always sent first. If the repetition period of the master multivibrator is somewhat longer than the sonic transit time, it will be true for the second channel also since the sound is received before any new noise is generated. However, for temperature measurement it is necessary to snychronize T_1 with the received signal from R_1. The time necessary for the noise from T_1 to die down to a level below that necessary for the level selecting circuit of R_2 to be able to detect the signal from T_2 (instead of the noise from T_1), is considerable longer than D_1, the wind delay. This difficulty is removed by adding an additional delay called the noise delay so both sound pulses can be received before any new noise is generated. The noise delay circuit is composed of tubes V7 and V6B. The noise delay signal is shown as waveform 9. Note that the negative going portion of the master multivibrator (waveform 1) is synchronized by the end of the noise delay.

The theory shows that the wind information is available as the difference in the sonic transit time. The

temperature information on the other hand is contained in the total roundtrip time and is available, therefore, only on alternate cycles operation. The alternate pulse selection is accomplished by a gate signal generated by a delay multivibrator circuit comprising tube V28 and associated components. The signal from this circuit is shown as waveform 18. The gate circuit, V25B controlled by waveform 18, serves to select alternate sweep triggers of waveform 17 which are derived from receiver 1 level selecting Schmitt circuit V12. These alternate wind triggers are combined with the temperature triggers of waveform 15 in cathode follower V29 to provide a composite trigger waveform 19 for the scope, thereby causing the scope to be triggered alternately by the wind trigger and temperature trigger. Waveform 12 is also fed to the vertical amplifier of the scope to cause the temperature trace to be displaced vertically from the wind trace.

Signals from the pulsed oscillator and decimal divider counters which make up the precision long time delay are shown as waveforms 13, 14, 15, and 16. Waveform 13 is the putput of the pulsed oscillator. Note that it is started at the same time that T_1 is fired. Waveform 14 shows the shaped pulses from the oscillator and waveform 15 represents the output from the two Berkeley counters. In this waveform the number of pulses that appear will depend on the preset position of the counters. Waveform 15

is the output of the long delay which is used to trigger the synchroscope temperature sweep as discussed in the last paragraph. As previously mentioned waveform 12 provides the signal which displaces the Y axis position of the temperature signal to separate it from the wind signal. If separate synchroscopes (and cameras for recording) are used this signal is unnecessary.

Photos of the three basic units are shown in Figures 1 - 4, 7 and 8.

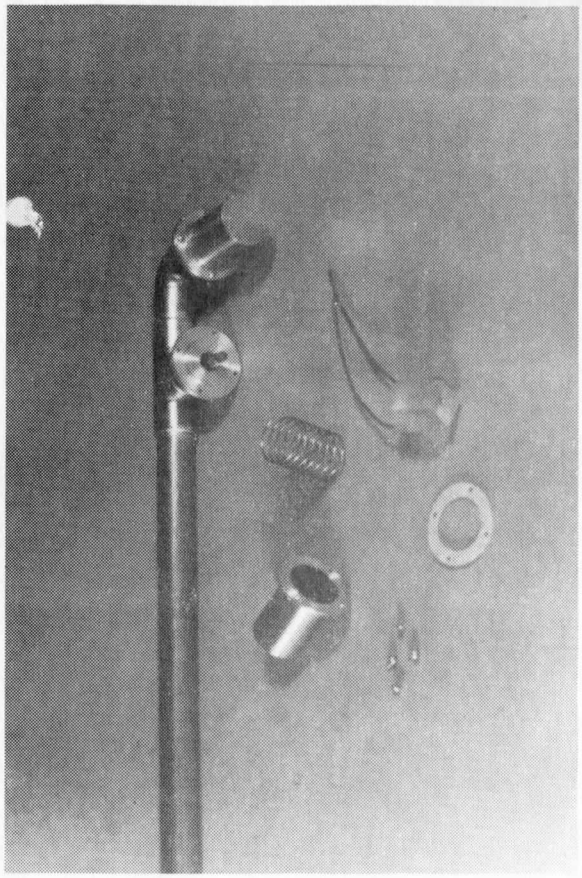

Fig. 1

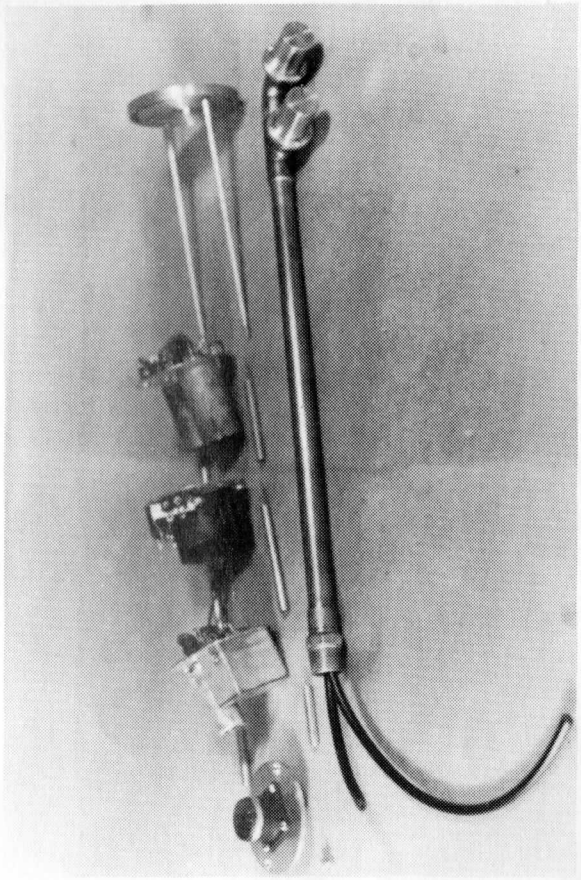

Fig. 2

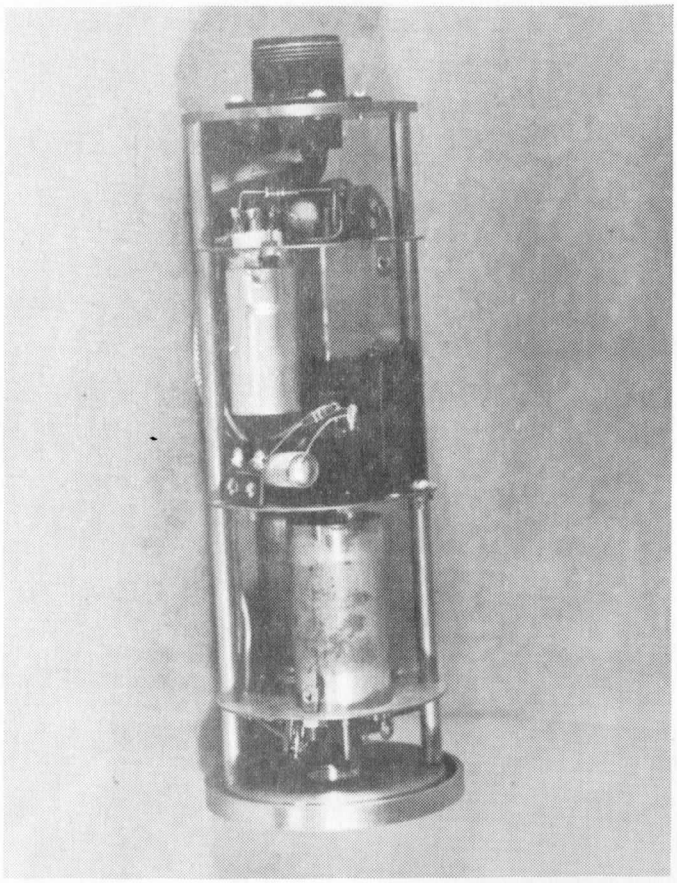

Fig. 3

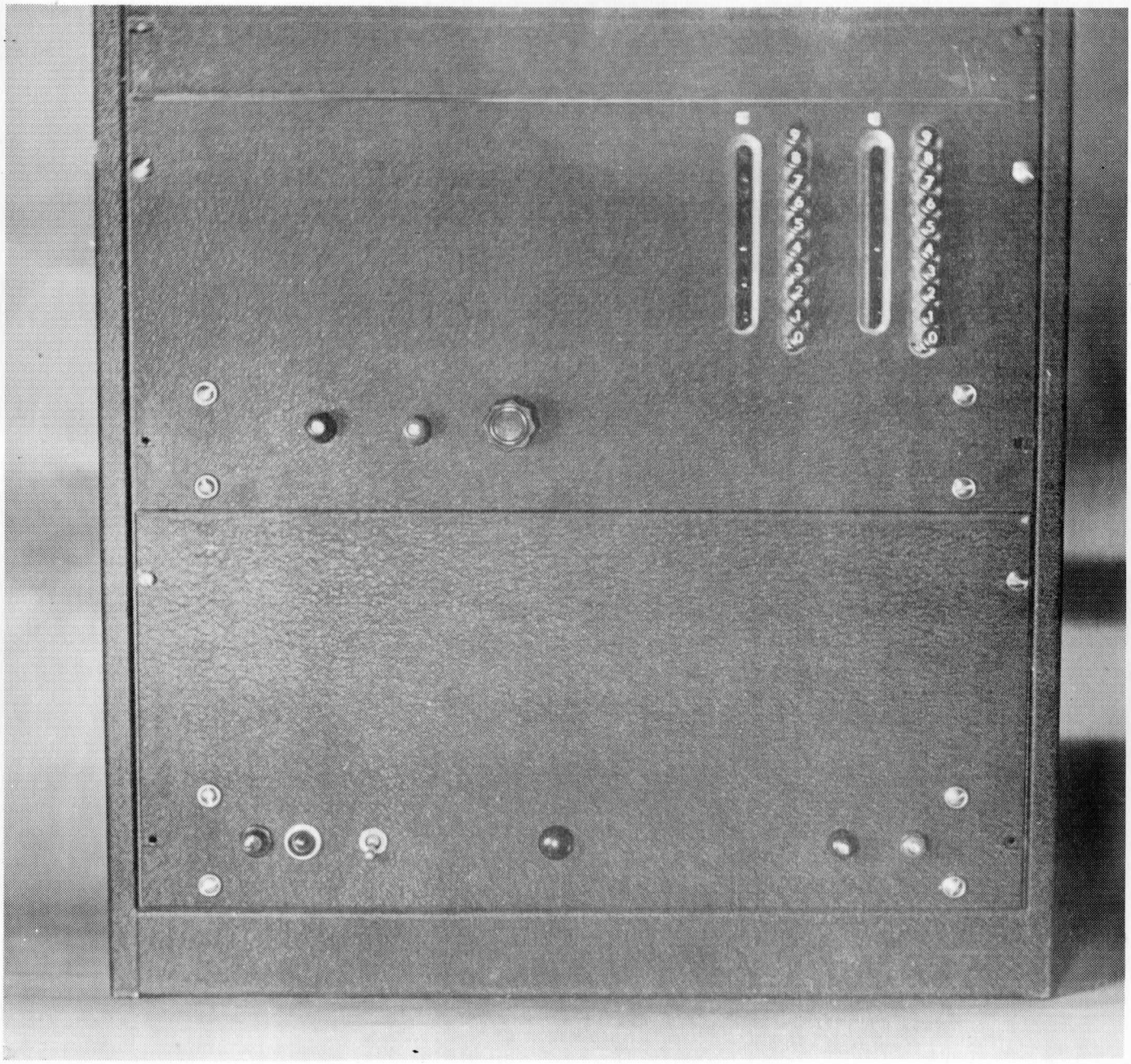

Figure 4

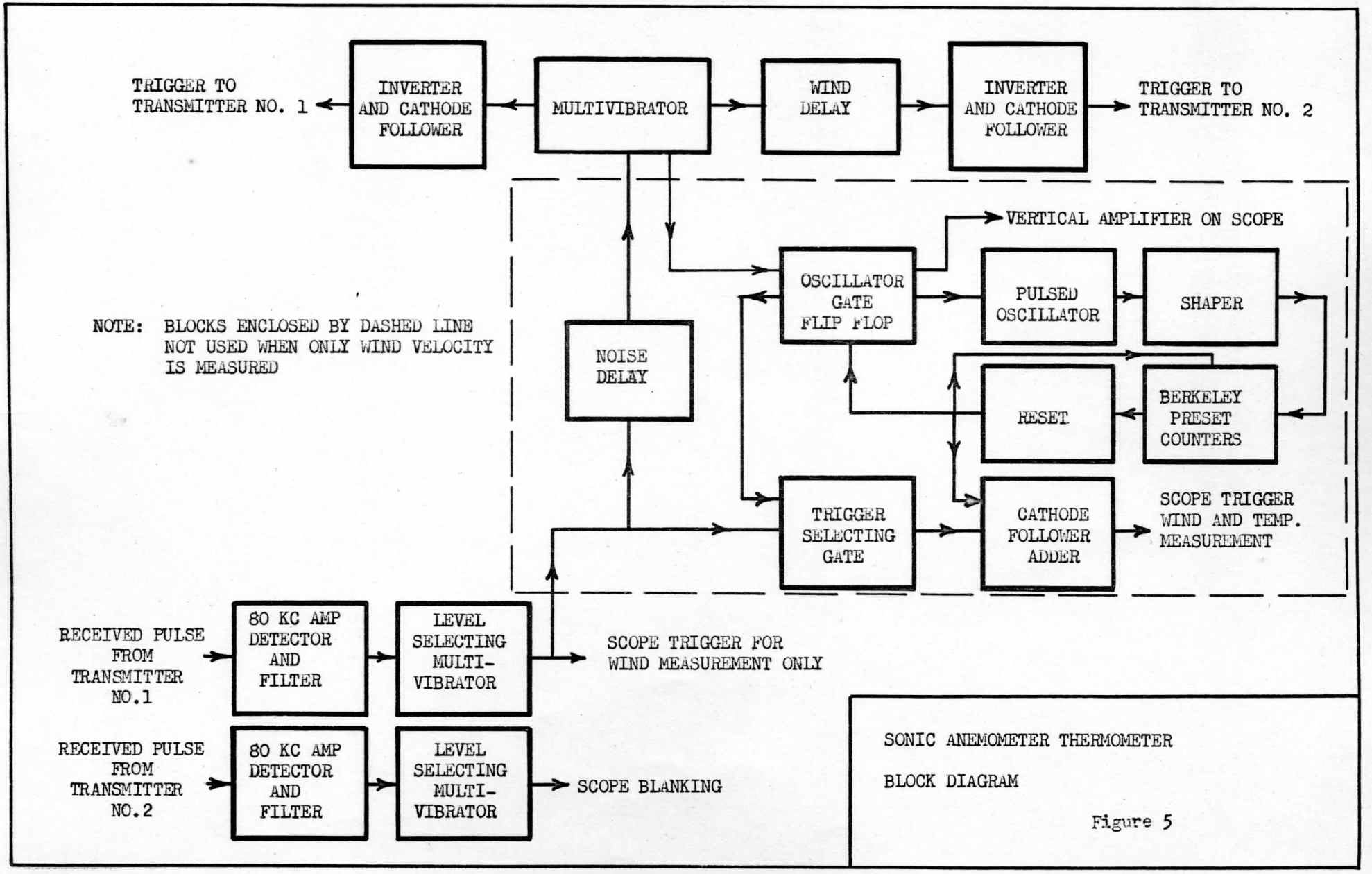

SONIC ANEMOMETER THERMOMETER

BLOCK DIAGRAM

Figure 5

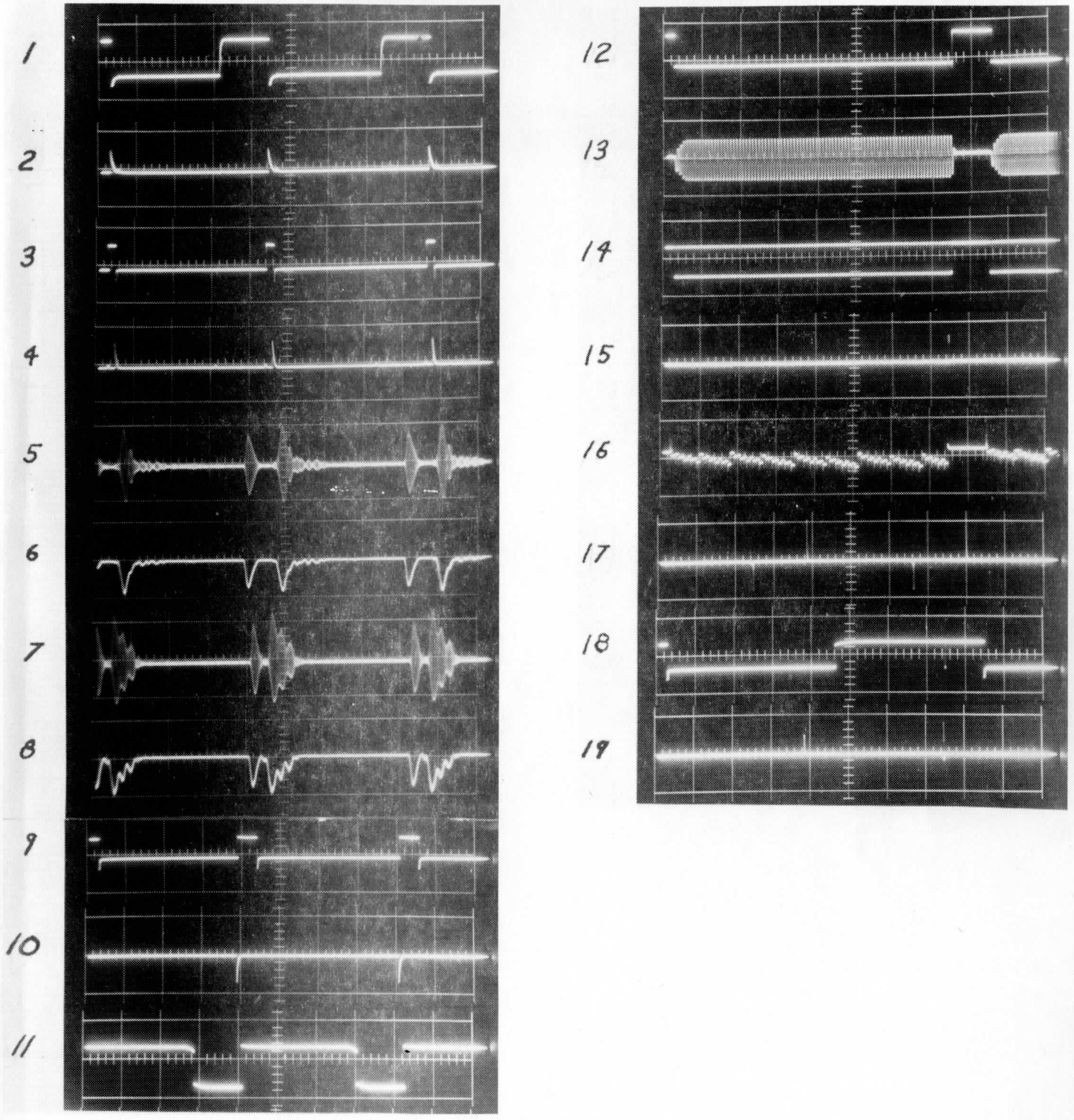

Figure 6

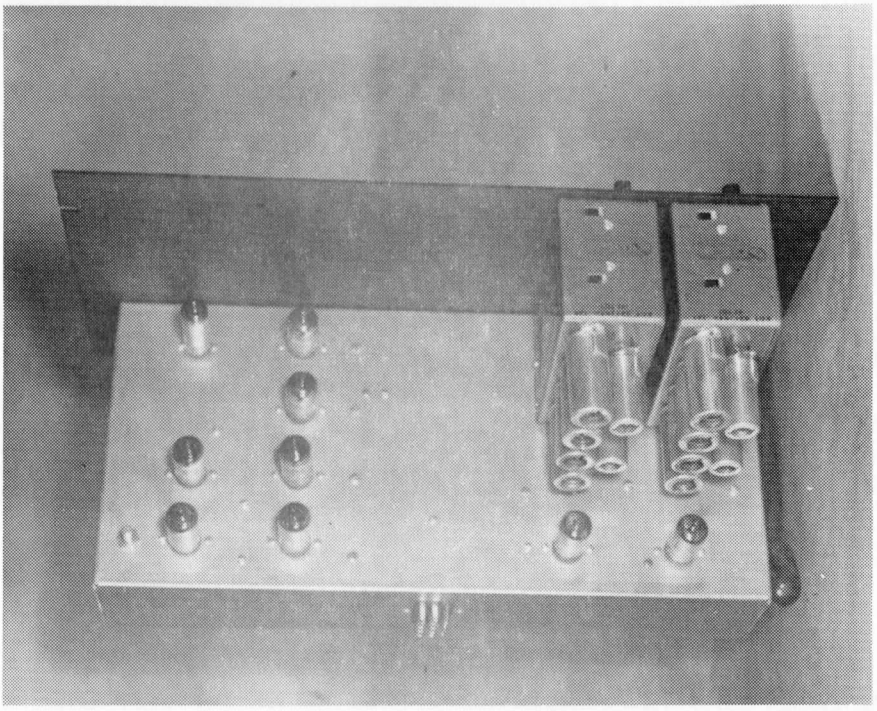

Figure 7

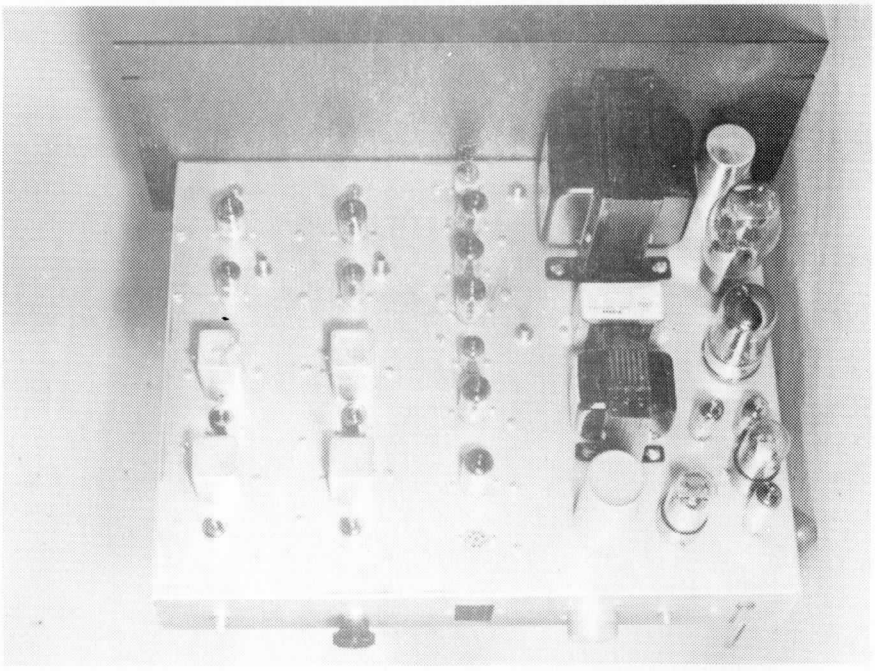

Figure 8

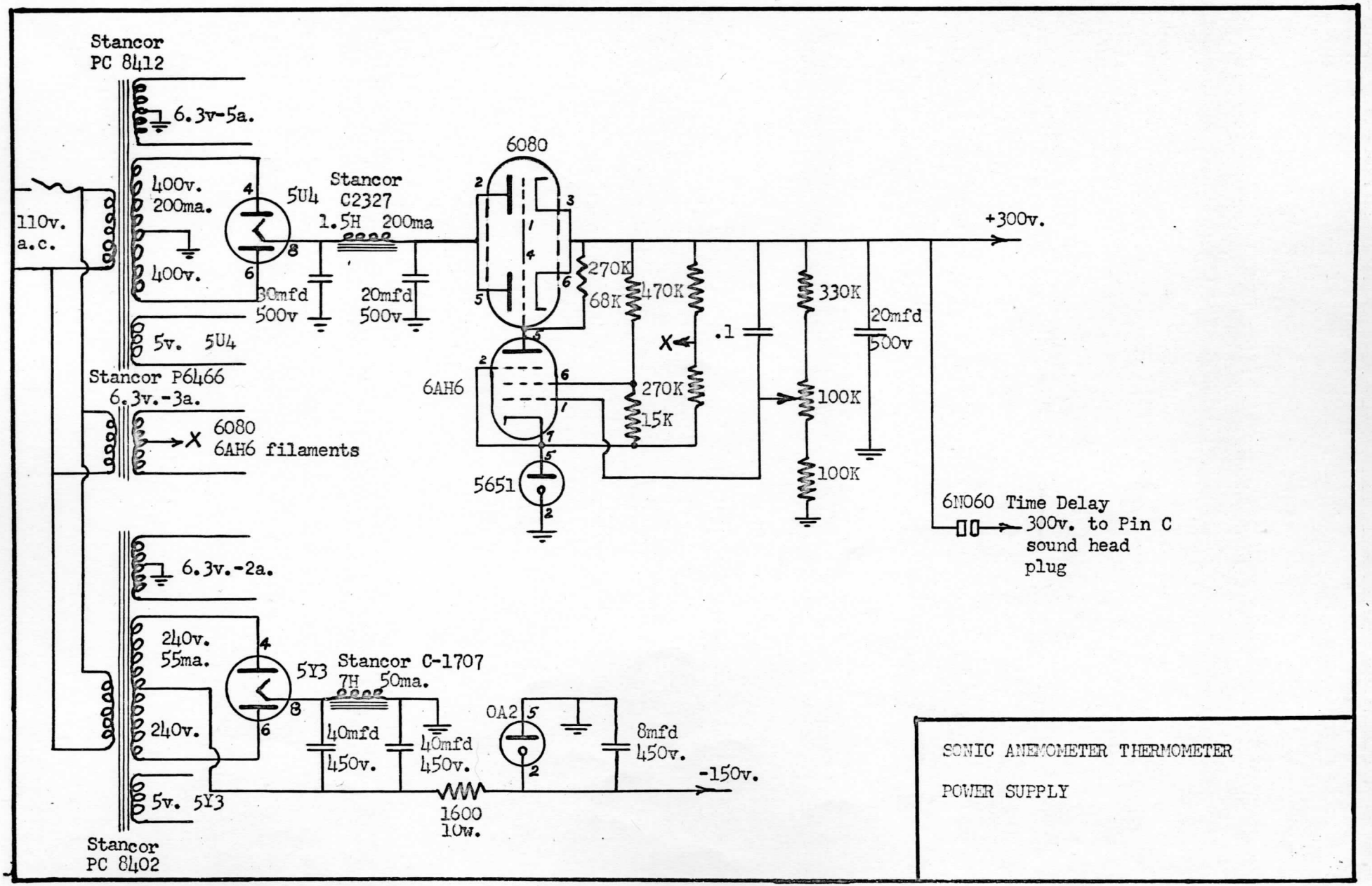
Stancor
PC 8412
6.3v-5a.
110v.
a.c.
400v.
200ma.
400v.
5v. 5U4
5U4
Stancor
C2327
1.5H 200ma
30mfd
500v
20mfd
500v
6080
+300v.
270K
68K
470K
.1
330K
20mfd
500v
100K
100K
6AH6
270K
15K
5651
Stancor P6466
6.3v.-3a.
6080
6AH6 filaments
6N060 Time Delay
300v. to Pin C
sound head
plug
6.3v.-2a.
240v.
55ma.
240v.
5v. 5Y3
5Y3
Stancor C-1707
7H 50ma.
40mfd
450v.
40mfd
450v.
1600
10w.
0A2
8mfd
450v.
-150v.
Stancor
PC 8402
SONIC ANEMOMETER THERMOMETER
POWER SUPPLY

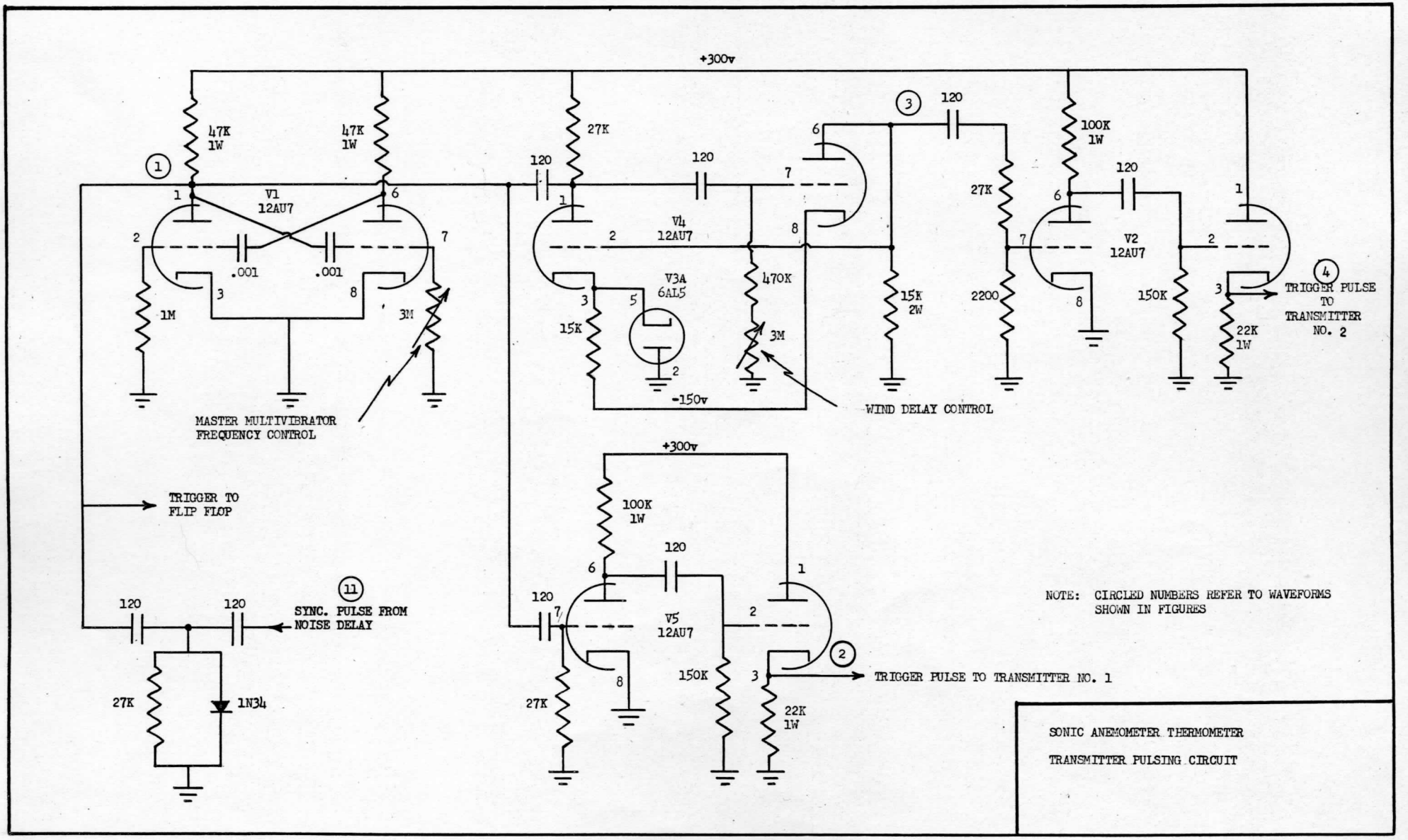
+300v
47K 1W
47K 1W
27K
120
120
120
100K 1W
V1 12AU7
V4 12AU7
V2 12AU7
V3A 6AL5
.001
.001
1M
3M
470K
15K
15K 2W
2200
150K
22K 1W
MASTER MULTIVIBRATOR FREQUENCY CONTROL
WIND DELAY CONTROL
TRIGGER PULSE TO TRANSMITTER NO. 2
-150v
TRIGGER TO FLIP FLOP
SYNC. PULSE FROM NOISE DELAY
27K
1N34
V5 12AU7
TRIGGER PULSE TO TRANSMITTER NO. 1
NOTE: CIRCLED NUMBERS REFER TO WAVEFORMS SHOWN IN FIGURES
SONIC ANEMOMETER THERMOMETER
TRANSMITTER PULSING CIRCUIT

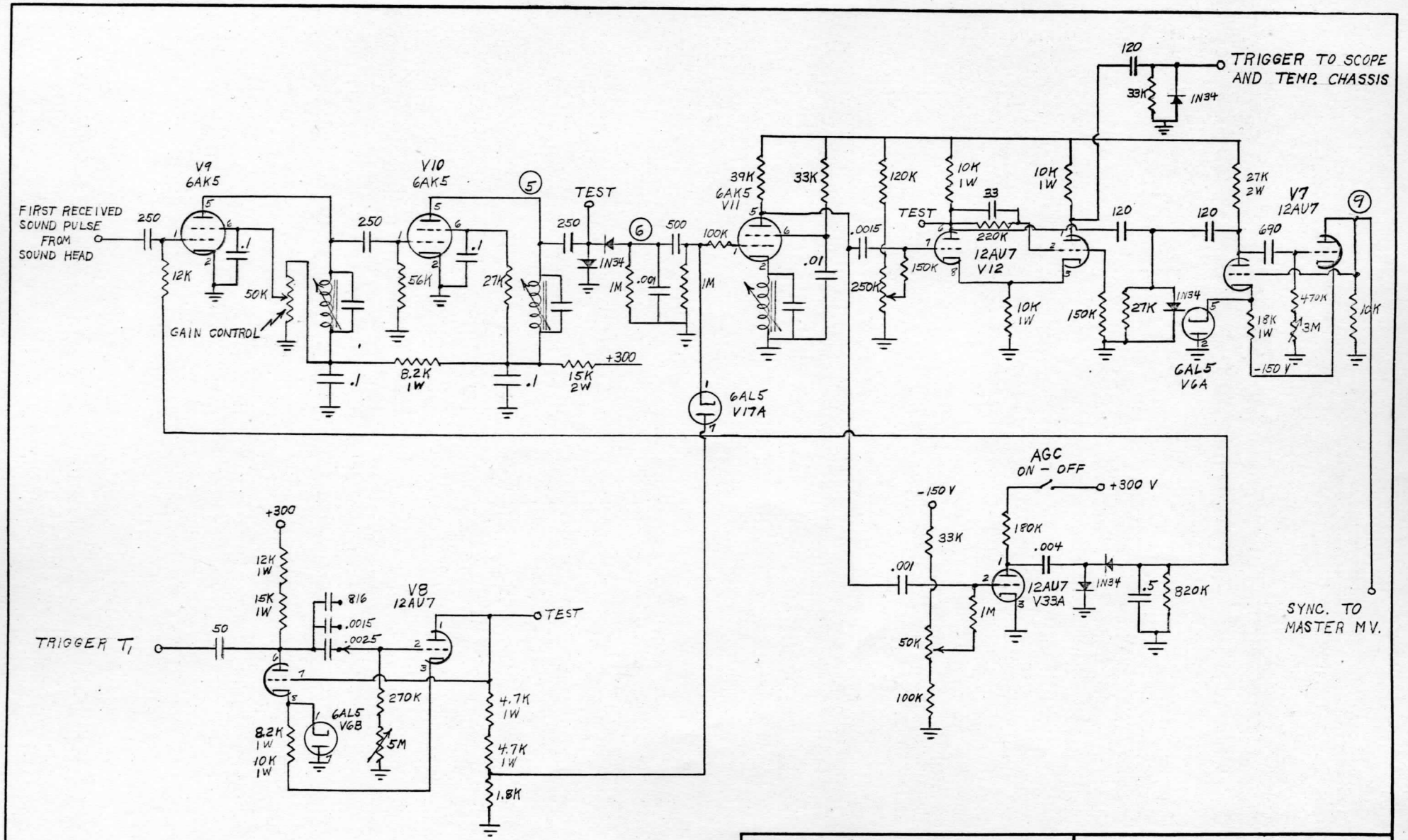

Capacitors in mfds in decimals, whole numbers mmfd		UNLESS OTHERWISE NOTED
Resistors in ohms ½w, 10%		
Dr. H H M	Eng. H H M	Date 3/15/57
Dwg. No.		

UNIVERSITY OF WISCONSIN
Electrical Standards and Instrumentation Laboratories

SONIC ANEMOMETER THERMOMETER

FIRST RECEIVED SOUND PULSE AMPLIFIER AND AGC CIRCUIT

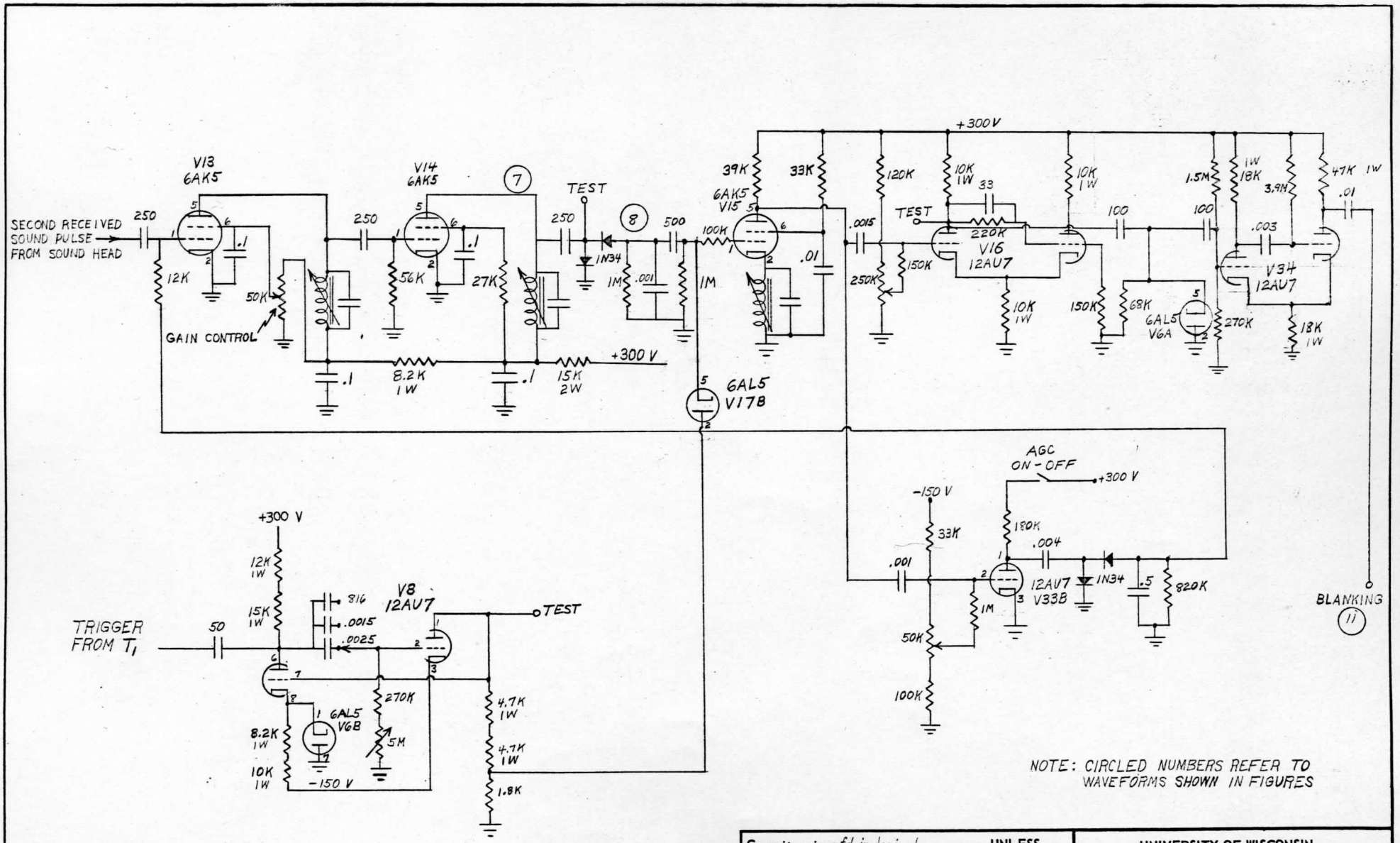

Capacitors in mfd. in decimals, whole numbers mmfd			UNLESS OTHERWISE NOTED
Resistors in ohms ½w, 10%			
Dr. H.H.M.	Eng. H.H.M.	Date 3/15/57	
Dwg. No.			

UNIVERSITY OF WISCONSIN
Electrical Standards and Instrumentation Laboratories

SONIC ANEMOMETER THERMOMETER
SECOND RECEIVED SOUND PULSE AMPLIFIER AND AGC CIRCUIT

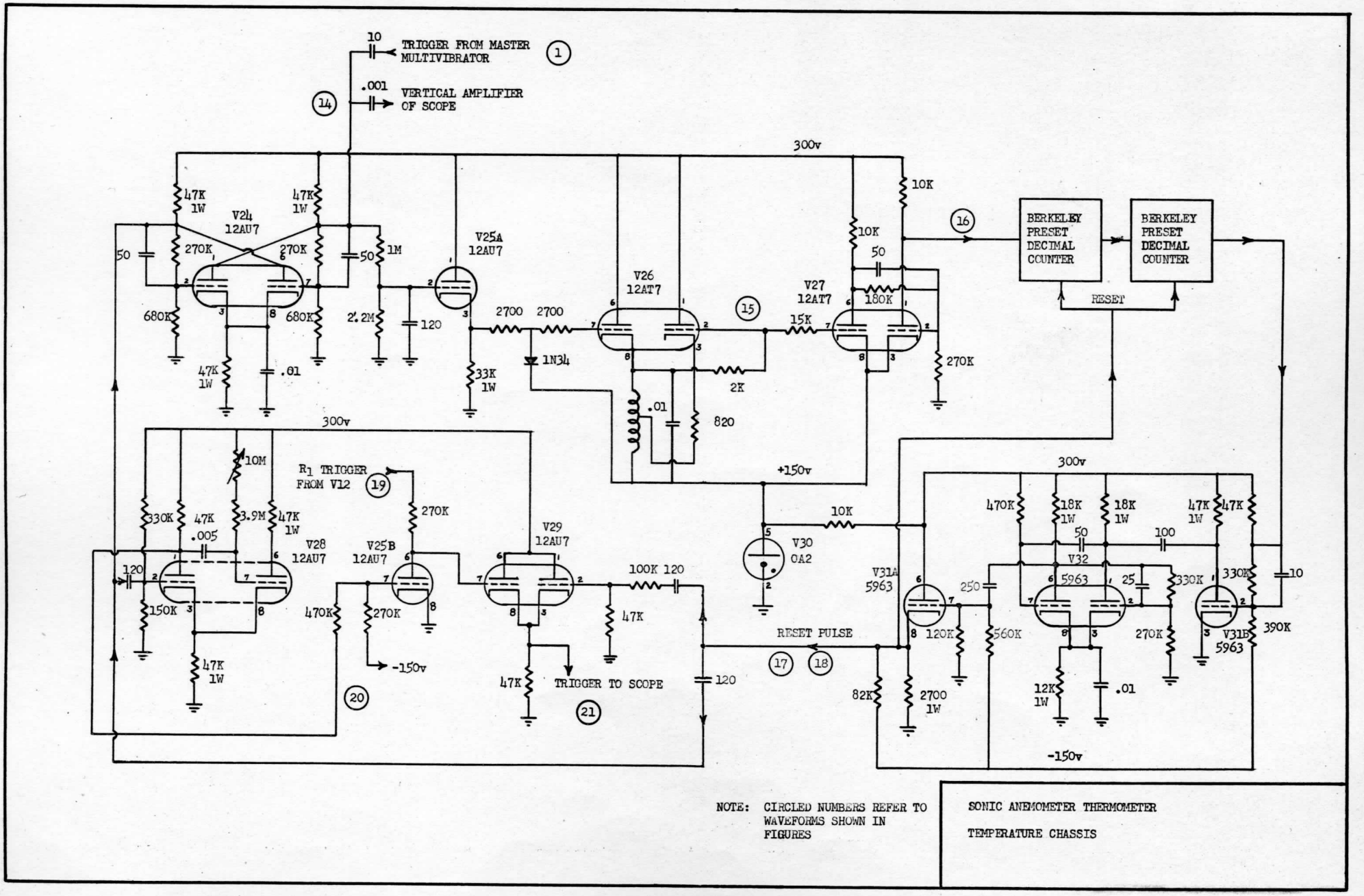

NOTE: CIRCLED NUMBERS REFER TO WAVEFORMS SHOWN IN FIGURES

SONIC ANEMOMETER THERMOMETER

TEMPERATURE CHASSIS

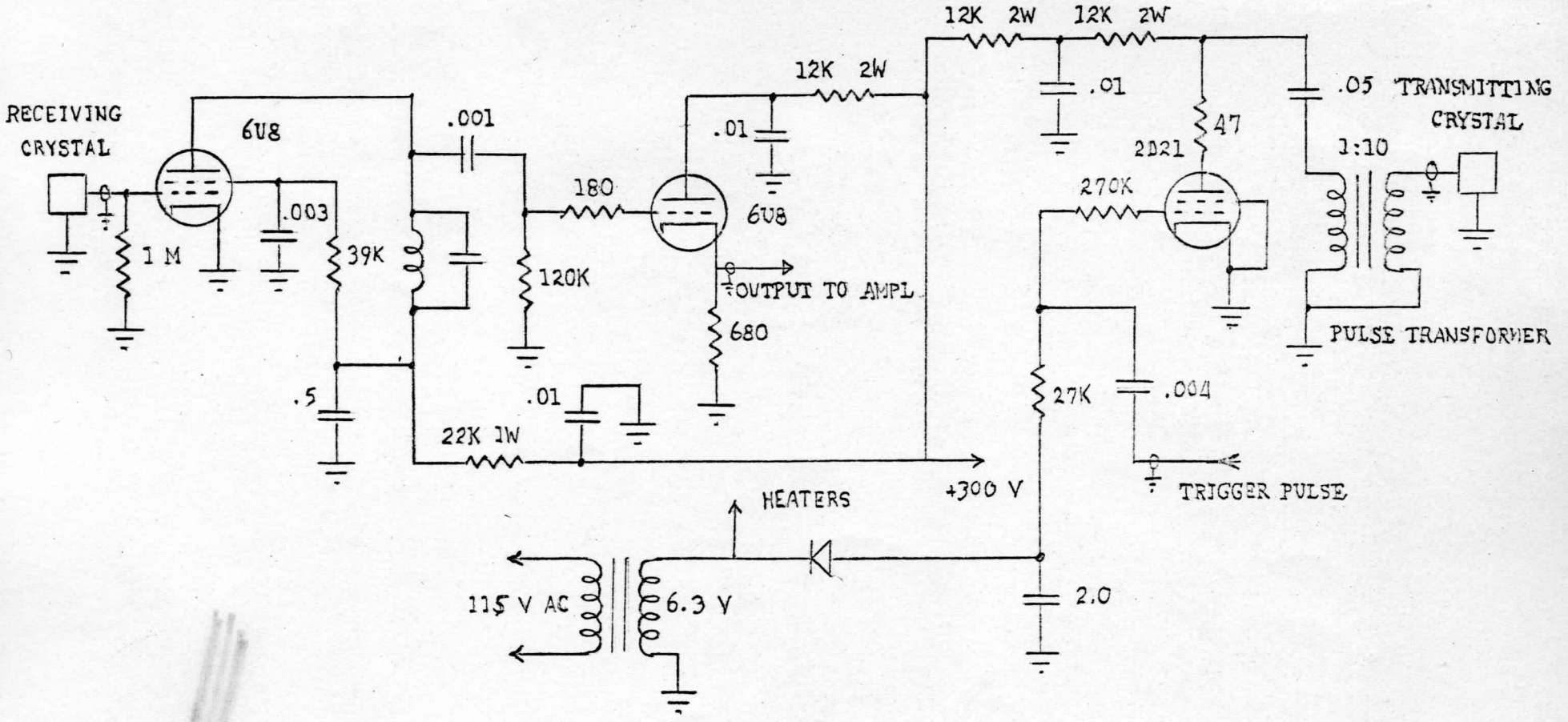

Capacitors in mfd Resistors in ohms ½w, 10%		UNLESS OTHERWISE NOTED
Dr. E.H.S.	Eng. H.H.M.	Date 3/15/57
Dwg. No. Figure 4		

UNIVERSITY OF WISCONSIN
Electrical Standards and Instrumentation Laboratories
RECEIVER AND TRANSMITTER HEADS
SONIC ANEMOMETER THERMOMETER